TECHNICAL REPORT

ISO/TR 23602

First edition
2005-07-01

Toughness of chain steels

Résistance des aciers pour chaînes

Reference number
ISO/TR 23602:2005(E)

ISO copyright office
Case postale 56 • CH-1211 Geneva 20
Tel. + 41 22 749 01 11
Fax + 41 22 749 09 47
E-mail copyright@iso.org
Web www.iso.org

Published in Switzerland

Contents

Page

Foreword

ISO (the International Organization for Standardization) is a worldwide federation of national standards bodies (ISO member bodies). The work of preparing International Standards is normally carried out through ISO technical committees. Each member body interested in a subject for which a technical committee has been established has the right to be represented on that committee. International organizations, governmental and non-governmental, in liaison with ISO, also take part in the work. ISO collaborates closely with the International Electrotechnical Commission (IEC) on all matters of electrotechnical standardization.

International Standards are drafted in accordance with the rules given in the ISO/IEC Directives, Part 2.

The main task of technical committees is to prepare International Standards. Draft International Standards adopted by the technical committees are circulated to the member bodies for voting. Publication as an International Standard requires approval by at least 75 % of the member bodies casting a vote.

In exceptional circumstances, when a technical committee has collected data of a different kind from that which is normally published as an International Standard ("state of the art", for example), it may decide by a simple majority vote of its participating members to publish a Technical Report. A Technical Report is entirely informative in nature and does not have to be reviewed until the data it provides are considered to be no longer valid or useful.

Attention is drawn to the possibility that some of the elements of this document may be the subject of patent rights. ISO shall not be held responsible for identifying any or all such patent rights.

ISO/TR 23602 was prepared by Technical Committee ISO/TC 111, *Round steel link chains, chain slings, components and accessories*, Subcommittee SC 1, *Chains and chain slings*.

Toughness of chain steels

1 Scope

The objective of the investigation presented in this Technical Report was to quantify the required material toughness for the operational safety of round steel chains. The determination of this toughness must take place under unfavourable boundary conditions, i.e. at the lowest permissible operating temperature on damaged (precracked) chains. On the basis of characteristic properties determined on chains and three-point bend (TPB) specimens and the notch impact energy, a load-bearing and brittle fracture transition temperature concept was elaborated. From the correlation of the fracture stress of chains, fracture mechanics characteristic properties and the notch impact energy, minimum values of the notch impact energy can be derived which yield adequate safety against fracture for the damaged chain. Furthermore, in order to exclude brittle failure of chains, the position of the lowest permissible operating temperature relative to the NDT (nil-ductility transition) temperature was determined. Finally, the linkage of the determined fracture mechanics properties to notch impact energy values and the definition of the requirements for these values furnishes a simple test and acceptance procedure for chain materials and chain types.

2 Normative references

The following referenced documents are indispensable for the application of this document. For dated references, only the edition cited applies. For undated references, the latest edition of the referenced document (including any amendments) applies.

ISO 3077:2001, *Short-link chain for lifting purposes — Grade T, (types T, DAT and DT), fine-tolerance hoist chain*

ISO 16872:—[1)], *Short link chains for lifting purposes — Grade VH, fine tolerance for manually operated chain hoists*

ISO 16877:—[1)], *Short link chains for lifting purposes — Grade TH, fine tolerance for manually operated chain hoists*

DIN 17155, *Steel for welded round links; technical delivery conditions*

EN 10083-3, *Quenched and tempered steels — Part 3: Technical delivery conditions for boron steels*

EN 10002 (all parts), *Metallic materials — Tensile testing*

EN 10045 (all parts), *Metallic materials — Charpy impact test*

BS 5762, *Methods for Crack Opening Displacement (COD) Testing*

ASTM E 813, *Standard Test for Jic, A Measure of Fracture Toughness*

ASTM E 399, *Standard Test Method for Plane-Strain Fracture Toughness of Metallic Materials*

1) Under preparation.

3 Types of chain and extraction of specimens

For the investigation, chains of size 16 × 48 were selected. The diameter of 16 mm and the length of the straight shank are suitable for the extraction of notch impact bend and three-point bend specimens for fracture mechanics tests, as well as small standard tensile test specimens. For fracture mechanics tests of the chains themselves, the unwelded shank was notched on the inner side. The test cross-section is thus the same for the chain specimen, the notch impact bend specimen and the standard tensile specimen — which means that in all cases the testing is based on the same material and heat-treatment conditions.

The 16 × 48 chains were manufactured to conform with ISO 3077:2001, Type T, ISO 16877:—[2)] , Grade TH and ISO 16872:—[2)], Grade VH. Thus chains which may be employed in all hoists (Type T) and exclusively in hand-operated hoists (Grade TH and Grade VH) are dealt with. Corresponding to their designation, the chains have a minimum nominal fracture stress of 800 and 1000 N/mm^2.

4 Materials, chemical composition and heat-treatment

The materials requirements for the manufacture of the chains involved in the investigation are given in Table 1. Chains conforming to ISO 3077, Type T shall have the minimum contents given in Table 1 as regards the alloying elements Ni and Cr and/or Mo. Furthermore, the Al and the upper limits for P and S content are specified.

For both chain types for use in hand operated hoists merely an Al content > 0,025 and limits of P and S to 0,025 and 0,020 respectively are called for. In the lower part of Table 1, the product analyses for the individual chain specimens are given. A comparison with the specified values shows that all materials meet the requirements of the corresponding International Standard in every respect. For the material investigated for chains conforming to ISO 3077, a triple alloyed steel designated 23MnNiCrMo53 in DIN 17115 is invoked. The two chains of Types TH and VH were made of a manganese-boron steel of European manufacture. The steel is 19MnB4+Cr conforming to EN 10083-3.

All of the chains investigated underwent an induction heat-treatment. They were austenitised inductively at 1 050 °C and water quenched. Subsequently, conventional tempering took place in an air circulation furnace under the following conditions:

ISO 3077:2001, Type T: 440 °C/ 2 h

ISO 16877:—[2)], Grade TH: 365 °C/ 2 h

ISO 16872:—[2)], Grade VH: 180 °C/ 2 h

5 Tensile tests on chains

The round steel chains selected for the tests had not been subjected to the manufacturing proof force, by which the chains are stressed beyond their elastic limit such that in certain regions yield occurs and residual stresses arise. In subsequent tests, these residual stresses would have affected the determined material characteristic properties and especially their dependence on notch depth, in a manner which would not have been able to be understood. For this reason, the application of the manufacturing proof force was dispensed with. The tensile tests were carried out on the one hand at room temperature with 5-link specimens as in the corresponding chain standards and on the other hand at the lowest permissible operating temperature of –40 °C. Since these low-temperature tests were carried out with the same gripping arrangements as with the fracture mechanics tests on notched and slit specimens, the testing was performed at –40 °C on 3-link specimens. This is of no importance, since the total ultimate elongation at fracture values is irrelevant due to the missing application of the manufacturing proof force. They were carried out nevertheless in order to obtain a starting point as to what deformation capacities the individual chains possessed.

2) Under preparation.

Table 2 gives the requirements for breaking force at room temperature in accordance with the appropriate standards and the fracture stress resulting therefrom as well as the requirements for total ultimate elongation A. From this it can be seen that the requirements for fracture stress of chain to ISO 3077, Type T and chain to ISO 16877:—[2)], Grade TH, are greater than 800 N/mm^2 and for chain to ISO 16872:—[1)], Grade VH, greater than 1 000 N/mm^2.

The required minimum total ultimate elongation values range from > 10 % for the Type T chain to > 17 % for the Grade VH chain. In the lower part of Table 2 the values determined on the chains are given. All the minimum requirements are exceeded by a large margin. At room temperature the Type T chain attained a fracture stress of 902 N/mm^2, while the Grade TH and Grade VH chains reached 806 N/mm^2 and 1 034 N/mm^2, respectively. This indicates that the strength of the Grade TH and VH chains made of manganese-boron steel only slightly exceeds the required values. The total ultimate elongations of between 33 % for the Type T chain and 40 % for the Grade TH chain show that the deformation capacity of the individual chain links is relatively large. The fracture stress values determined at –40 °C do not differ significantly from those at room temperature for the Type T and Grade TH chains. The Grade VH chain shows a fall-off which is, however, entirely attributable to the surface. On removal of the –40 °C cold chain from the cold chamber, the surface of the chain immediately became coated with hoarfrost. This frost led to significant reduction of the friction between the chain links. This effect influences the fracture stress of the chain as the material strength increases.

The core hardness values of the chains tested are also given in Table 2. In all cases these correspond with the determined chain strengths. In all the tensile tests at both test temperatures, the chains failed in the rounded end.

6 Conventional tensile tests on standard specimens

For the performance of tensile tests conforming to EN 10002, tensile specimens of size 6 × 30 were taken from the unwelded shanks of the chain links. The specimens were short-proportioned with threaded heads. These specimens were tested at the lowest permissible operating temperature of –40 °C. Almost identical results resulted for the 0,2 % yield stress $R_{p0,2}$ and ultimate tensile strength R_m for both Type T and Grade TH chains. The yield stress is about 1 150 N/mm^2 and the tensile strength R_m about 1 240 N/mm^2, see Table 3. The same applies for the deformation values, the elongation % A_5 and the reduction of area Z where the A_5 values are about 14 % and the Z values at about 65 %. As may be expected, the material of the Grade VH chain deviates from the above showing a higher 0,2 % yield stress of 1 260 MPa and a tensile strength R_m of 1 430 MPa. Corresponding to the higher strength here, the elongation at fracture is 12 % and the reduction of area 60 %.

The ratios of the material tensile strength to the breaking strength of the chain lie at mean values of 1,46 for Grade TH and Type T chains and 1,36 for Grade VH chain. Accordingly, this correlation varies within the usual bounds [1].

7 Notch impact tests

For the performance of the notch impact tests ISO V (Charpy-V), specimens conforming to EN 10045 or ISO/R 442[7] with V notches were taken from the unwelded shanks of the chain links. The tests were carried out over a temperature range of –80 °C to +80 °C. During every impact test a record of the force-time history was obtained by means of an instrumented 300 J pendulum impact testing machine to the striker of which resistance strain gauges were attached. The results are given in Table 4 and are shown in Figure 1 as K_V - temperature curves. All 3 chain types tested showed a marked transition temperature behaviour. For the specimens from Type T chain, the transition temperature range lies between –40 and room temperature. For both the manganese-boron steel chains, however, the transition range is shifted to higher temperatures of about 0 °C to +80 °C.

On the upper shelf, specimens of Type T chain reached values of about 105 J, those of Grade TH about 80 J, and those of Grade VH about 55 J. The determined values show good agreement with those obtained for the same and similar materials and in published results [1] and [2].

More precise information on the brittle fracture transition behaviour of the individual materials can be obtained from the instrumented notch impact test. Correlations of the crack arrest force in the notch impact test with the NDT temperature determined in the Pellini drop-weight test show that the temperature at which a crack arrest force of 4 kN occurs corresponds to a wide extent to the NDT temperature [3],[4]. Examples of force–time diagrams are shown in Figure 2. According to Figure 2a), no crack arrest occurs at a test temperature of –40 °C in a Type T specimen. On raising the test temperature by 10 K, crack arrests occur at a force of 4 kN, see Figure 2b). If, on the other hand, the specimen is tested on the upper shelf, no rapid crack growth occurs. This may be seen from Figure 2c) at a test temperature of 20 °C.

The evaluation of all the notch impact tests carried out in the transition region for the 3 materials investigated are summarised in Table 5 and Figure 3. From the curves NDT temperatures of –30 °C, +17 °C and +22 °C result respectively for the Type T, Grade TH and Grade VH materials. Consequently, the crack arrest force and thus the NDT temperatures of the Grade TH and VH chains do not differ significantly. They lie at room temperature, which means that cracked chains of these qualities can only just arrest cracks.

Another method of determining the brittle fracture transition temperature can also be carried out without instrumentation of the impact testing machine. In this, an evaluation is made of the fracture surfaces of notch impact specimens with regard to the proportion of ductile fracture. This proportion is related as a percentage of the total fracture surface and plotted against test temperature. The criterion for the brittle fracture transition is 50 % ductile fracture (FAT temperature).

The results for the investigated chains assessed in this manner are +30 °C for Grades TH and VH and –25 °C for Type T, see Table 6 and Figure 4.

In Table 7 the determined brittle fracture transition temperatures for all the chains using both methods are summarised. The values for the Type T chain show relatively good agreement of the NDT and FAT temperatures, whereas the NDT temperatures for the Grade TH and VH chains lie about 10 K lower than the FAT temperatures. The more reliable method for determination of the brittle fracture transition temperature is the instrumented notch impact test. Here the NDT temperature is determined by means of objective characteristic values. The FAT temperature, on the other hand, rests on the subjective estimation of the brittle or ductile fractions of the fracture surface.

The NDT temperatures of +17 and +22 °C determined for the manganese-boron steels agree exactly with the NDT temperature determined in earlier work on a manganese-boron steel chain of Category 100. Here likewise a value of +20 °C was determined from the instrumented notch impact test [1].

8 Fracture mechanics tests on notched chain links with slits

For the determination of fracture mechanics characteristic properties, 3-link specimens were selected in which the middle link was notched on the inner side of the unwelded shank and subsequently fatigued. From this fatigue, cracks with irregular crack fronts resulted. In contrast to the elliptical crack fronts arising in the normal case, here the crack advanced much further in the centre of the specimen. This crack advance at the specimen centre was so great in comparison to that at the edge of the specimen that a fracture mechanics evaluation of the specimens was not possible. Furthermore, detection of the fatigue crack depth was extraordinarily difficult. In particular, the cut-off of the resonance test equipment via the drop-off in frequency is ruled out since the chain link forms a closed ring and thus with advancing crack the frequency drop-off is extremely small. A possible solution for the introduction of fatigue cracks which are amenable to fracture mechanics evaluation would perhaps be offered by a circumferential notch in the test cross-section with the use of the potential probe measurement technique for determination of the crack depth.

For the creation of absolutely reproducible relationships with respect to crack depth and crack front, very narrow slits were introduced into the chain links by wire spark erosion. For this a fine wire with a diameter of 0,15 mm was employed which produced slit widths of 0,25 mm and slit tip radii of 0,125 mm. In metallographic sections through the slit tip, no thermally induced structural changes could be detected. Because of this slit tip radius of 0,125 mm, it is to be expected that in tough material conditions, no significant change occurs in load-bearing behaviour in comparison with a fatigue crack, since under load the crack tips are likewise considerably blunted (blunting). This expectation was confirmed by three-point bending specimens. With approximately the same crack depth to width ratios, the same force/COD plots were obtained.

The steeper path and higher peak load of the curve determined on the specimen with the fatigue crack can be attributed to the smaller crack depth, see Figure 5. Although, by the use of eroded slits in place of fatigue cracks with brittle material behaviour, higher failure loads are to be expected. This was likewise confirmed on three-point bend specimens of Grade VH material, see Figure 6. It is seen that in the brittle material condition, the failure load of the fatigue crack lies 20 % below that of the eroded slit. The differing gradients of the two load COD curves are again attributable to the differing crack depths. If one corrects for the crack depth, an approximately 25 % difference in the fracture load results. A comparison of fatigued and slit chain links led to the same failure force relationships as in the bending specimens. Here the breaking force of the fatigued chain link also lies 25 % below that of the chain link with a slit, see Figure 7.

This comprehensible agreement or reproducible deviation in all cases justifies the introduction of eroded slits in the test chains and permits a later correction of the results. For the systematic investigation of the influence of defect depth, 3 different defect depths were chosen. The depths of the eroded slits were 3,5 mm, 7,0 mm and 10,5 mm. These correspond to crack depth-diameter ratios of 0,22, 0,43 and 0,64, see Figure 8. For the determination of the crack opening on the inner side of the link shank, a COD clip gauge with applied resistance strain gauges was fastened to the chain link, see Figure 9. The relationship between the clip gauge opening and strain was calibrated using a micrometer screw, see Figure 10. Figure 11 shows a three-link chain specimen after the test at –40 °C, which shows the hoarfrost coating mentioned above. In conducting the tests, the force, testing machine displacement and crack opening were recorded. Examples of force–displacement and force–crack opening diagrams are shown in Annex 1.

The maximum loads as a function of the particular slit depth and the related elongations determined in the tests are summarised in Tables 8 and 9 respectively. The listed breaking force values are the averages of 4 individual values. Furthermore, the standard deviations for the particular 4 values are given. As is to be expected, the material with the highest notch impact energy, Type T, shows the smallest scatter, i.e the smallest standard deviation. It is noteworthy that the standard deviations of the breaking force values for all the materials are at a minimum for the crack depth ratio of 0,42. The overall relatively small standard deviation confirms the reproducibility of the eroded slits with respect to depth and shape.

The relationship between maximum load and relative defect depth is shown in Figure 12. Starting from the values of the defect-free chain, the maximum load falls off very sharply with a relative slit depth of 0,22, then with greater relative defects assumes an almost asymptotic path to specific value. This hyperbolic curve form can be attributed to the supporting effect of the second undefected shank of the chain. It is striking that for the chain specimens from the manganese-boron steel with the relative slit depth of 0,22 the maximum load has already fallen to half that for the slit-free specimen.

At larger relative slit depths the maximum loads of the chains of manganese-boron steel are only half those of Type T chain. Furthermore, it should be stressed that the curves of Grades TH and VH differ only to an insignificant extent. The small differences in the maximum load are even more astonishing if account is taken of the great difference in the material strength of the two chains and the widely different tempering temperatures. Both chains were hardened in the martensitic state. By contrast, the tempering temperatures of 180 °C for Grade VH and 365 °C for Grade TH differed widely. On the other hand, the notch impact energy of both material conditions is comparable. Thus the toughness is the dominant defining factor for the attainable maximum load of cracked or notched chains.

Typical Load–COD diagrams for the 3 slit depths and the 3 chains are shown in Figures 13, 14 and 15. These curves show that for Type T chain failure occurred by overload (plastic collapse). In order to check whether the collapse failure was preceded by crack initiation and stable crack growth, several chains were loaded up to differing maximal loads and the resulting stable crack growth therefore was detected by heat tinting (see example in Figure 16). For this reason, the fracture mechanics concept based on the COD and the J-integral were used for the quantification of the toughness behaviour of the Type T chain (see Clause 9). In contrast to this collapse behaviour, the fracture in the Grade TH and VH chains occurred in the linear elastic region. Consequently, the failure of these chains could be described by linear elastic fracture mechanics.

Along with the force and extension, the tensile tests on the chains were also evaluated with respect to the absorbed energy at fracture. These results are given in Table 10 and represented graphically in Figure 17. Here a hyperbolic curve of energy against relative slit depth also results in a drastic fall in energy which may be seen between the undamaged condition and the 0,22 relative slit depth. The energy is reduced by a factor of 20 for the Grade TH chain, by a factor of 25 for the Grade VH chain and by a factor of 4 for the Type T chain. Thus the absorbed energy at fracture at the relative slit depth of 0,22 in the Type T chain is three times

that in the Grade VH and TH chains. This relationship of a factor of 3 between the manganese-boron steel chains and the Type T chain also remains at greater relative slit depths. It is also noteworthy that at a relative slit depth of 1 the energy does not reduce to zero because the second shank takes over the load.

9 Fracture mechanics tests on notched three-point bend specimens with slits and fatigue cracks

9.1 Testing and evaluation technique

In the specimens having the dimensions of notch impact specimens as described in Clause 3, both spark-eroded slits and fatigue cracks with a crack depth ratio a/w = 0,5 were introduced. During the tests, the functions, force–bending deflection and force-crack opening (COD) were recorded. The specimen dimensions and testing arrangements can be seen in Figure 18. In addition, the geometry of the eroded slits is shown. The test evaluation took place in accordance with the COD and the J integral concepts, see Figure 19. Here the relationships between force and COD conforming with BS 5762 and between force and bending deflection in accordance with ASTM E 813 are shown schematically. In addition, the values V_p and U_{pl} required for the plastic evaluation are plotted. The formulae for the calculation of the fracture mechanics characteristic properties are given in Table 11. The elastic components δ_{pl} and J_{el} are calculated with the aid of stress intensity factor K_I. The plastic components result from the plastic crack opening – (V_p) and energy components (U_{pl}) which can be determined in correspondence with Figure 19. The total values δ_{tot} and J_{tot} result from the addition of the elastic and plastic components.

9.2 Tests on three-point bend (TPB) specimens with eroded slits

A three-point bend specimen was taken from each of the three types of chain investigated and tested at –40 °C. Both specimens from Grade TH and Grade VH chains failed in the linear elastic region while the specimen from Type T chain showed plastic collapse, see Figures 5 and 6. The fracture mechanics characteristic values calculated in accordance with the relationships in Table 11 are given in Table 12.

$$B, a, (W-a) \geqslant 2{,}5\left(\frac{K_Q}{R_{p0,2}}\right)^2$$

In ASTM E 399 two validity criteria are required to be met for linear elastic fracture mechanics tests. The specimens from Grade TH and VH chains meet the 5 % tangent criterion. However the size condition is barely fulfilled. For both types of chain, a K_Q value of about 3 000 N/mm$^{3/2}$ can be calculated. Corresponding to the largely linear elastic failure the J_{tot} and δ_{tot} values are very small. It emerges that the values of the specimen from the Grade VH chain with 50 compared to 45 N/mm for J_{tot} and 0,033 to 0,024 mm for δ_{tot} lie slightly higher. In the specimen from the Type T chain, the evaluation relates to the highest load point which more or less equates to stable crack initiation. The evaluation leads to a J_{tot} value of 149 N/mm and a δ_{tot} value of 0,106 mm.

The relationship between the crack tip opening (δ_{tot}) and the J integral (J_{tot}) is shown in Figure 20. There is an almost linear relationship between the two criteria. The sequence with respect to their toughness behaviour, of the chains investigated, becomes clear from the 3 to 4 times higher values of J and δ for Type T chain.

For the assessment of the effect of the eroded slits on the failure of the specimens, supplementary fatigued three-point bend specimens were tested at –40 °C. An overview of the properties so determined is given in Table 13. For the specimens from Grade TH and VH chains the K_Q values obtained from the eroded specimens are reduced from about 3 000 N/mm$^{3/2}$ to about 2 500 N/mm$^{3/2}$. It is still a matter of the K_Q value in which here, however, the size conditions are almost fulfilled. As expected, the δ values of the fatigued specimens are reduced by a factor of about 4 and the J values by a factor of about 2. Due to crack blunting the J and δ values for the specimen from the Type T chain are again of the same magnitude as for the slit specimens, see Figure 5.

In the described evaluations of the slit and fatigued specimens from the Type T chain, the peak load was always used which lies above the crack initiation force and in this case leads to excessive values. In order to obtain crack initiation, and thus conservative values, the initiation values for J and δ were therefore determined

on fatigued specimens of Type T chain using the multi-specimen technique. In this the extent of the stable crack growth was determined by use of the heat-tinting technique (see example in Figure 16). A total of three specimens were used, which were loaded to different levels and then unloaded again. A summary of all the characteristic properties determined in this manner is given in Table 14. The force–bending deflection and force–crack opening diagrams recorded in these tests are contained in Annex 2. Specimen 3-7 was loaded beyond collapse and despite this showed only the relatively small crack growth (Δa) of 0,25 mm. Accordingly, crack initiation and collapse are almost identical for this material. It should be pointed out that for the calculation of the U_{pl} value the specimen indentation (denting) was corrected. Figures 21 and 22 show the relationship between on the one hand the crack opening (Δa) and, on the other hand, the J integral and crack tip opening (R curve). The equations for the particular blunting lines result from these standards: in the case of J, according to ASTM 1820, as $J = 2 \times \sigma_{Fl} \times \Delta a$ and in the case of CTOD, according to BS 5762 as CTOD = $1.4 \times \Delta a$. The parallels to the blunting line through the crack extension Δa = 0,15 mm give the J and δ crack initiation values defined in the particular standard. For these values of J = 175 N/mm (Figure 21) and δ = 0,105 mm (Figure 22) the validity criteria for the appropriate standard are fulfilled. The further considerations are not based on the crack initiation values as defined above but rather on the real crack initiation values taken as the intersection of the blunting line and R curve in order to achieve, on the one hand, absolute conservatism for the tough material and, on the other, compatibility with data from the literature. The values which result from this as ductile fracture characteristic properties are J_i = 110 N/mm and δ_i = 0,065 mm, see Figures 21 and 22.

10 Correlation between the load-bearing capacity of chain links containing slits and material toughness

The relationship between the J integral and CTOD, and the gross area nominal stress of the chain containing slits, is shown in Figures 23 and 24. The gross area nominal stress results from the load at fracture divided by the sum of the gross cross sectional area of both of the chain link shanks.

Regressively derived families of curves linked the test points. This pattern results, at least in the elastic region, from the following expressions:

$$J = \frac{K_I^2}{E} = \frac{\sigma^2 \cdot \Pi \cdot a \cdot y^2}{E}$$

From this follows, according to the stress solved for constant crack depth, a:

$$\sigma = \sqrt{\frac{J}{c}}$$

where c is a constant.

The plotted fracture mechanics characteristic values are those which were determined on the three-point bend specimens with fatigue cracks. The J integral and CTOD values for the Type T chain are the initiation values taken from the R curves. With these diagrams in Figures 23 and 24 a link is made between the fracture mechanics characteristic properties determined on standard specimens and the load-bearing capacity of the damaged chain in the three quality classes investigated. From the above, the necessary fracture mechanics properties as a function of the particular defect depth for a required fracture stress of the chain can be successfully derived.

Corresponding with the objective of the investigation a similar relationship results in the correlation of the breaking load of the damaged chains with the notch impact energy (see Figure 25). The breaking load can be converted into the gross area nominal fracture stress from the relationship noted earlier (see Figure 26). Also from these graphs the necessary notch impact energy for a required load bearing capacity of the damaged chain with a given defect depth can be derived.

11 Fracture mechanics derivation of chain links

The computation of the stress intensity factor of a cracked component fracture mechanics requires the relationship between the defect size and the gross area nominal stress. In the case of a round steel chain

which is damaged on one side, i.e. on one shank, the derivation of the gross area nominal stress is not possible without something more, since in this case it concerns a statically indeterminate system in which it is not known how the applied force is distributed between the two shanks. In particular, the changing tensile and bending component of the stress with increasing crack depth is also unknown. To resolve these problems a systematic analysis using the finite element method (FEM) was performed using the ANSYS program. From this FE analysis, the longitudinal stresses as a function of crack depth shown in Figures 27 to 29 emerged. The division of the longitudinal stress into membrane and bending components leads to the representation given in Figure 30. For the crack-free chain, a ratio of bending stress, σ_b to membrane stress, σ_m of 2,2 results. This value was checked and confirmed by a stress analysis on the chain link using resistance strain gauges. The ratio of total stress to membrane stress was 3,1. This value for the stress elevation on the inner side of the straight shank of a round steel chain with a pitch to diameter ratio of 3 is known from earlier investigations.

In the literature [5] there is a solution for the calculation of the stress intensity factor K_I for a single-side cracked round bar under bending. The correction factor as a function of relative crack depth given in the above is shown in Figure 31. This solution was chosen since according to Figure 30 the bending stress is dominant in the chain link shank. As an example, the K_{IC} value was calculated for the slit Grade VH chain from the failure loads for various slit depths from the relationship given in Figure 31, Table 15. That the K_{IC} values as a function of slit depth differ only insignificantly and are on average at about 2 850 N/mm$^{3/2}$, speaks for the quality of this solution. Again this value agrees very well with the K_{IC} value of the slit three-point bend specimen of about 3 000 N/mm$^{3/2}$.

The relationship between stress intensity factor, relative defect depth and gross area nominal stress for a single side cracked round bar is shown in Figure 32. Likewise, in Figure 32 the calculated K_{IC} values from the breaking loads determined on the Grade VH chain are plotted, see Table 15.

$$K_I = \sigma_b \sqrt{\Pi \cdot a \cdot F_I}$$

Similar diagrams can be determined for other sizes and types of chain.

12 Load-bearing and brittle fracture transition concept — Requirements

Because the requirements on a fracture mechanics property for the guarantee of a sufficient chain fracture stress in the cracked condition lie in the elastic-plastic region, these requirements cannot be derived on the basis of Figure 32. However this is successfully achieved by including the determined J_i value.

In Figure 23 the relationship between the J_i values determined on fatigued bending specimens and the gross area nominal tensile stress of the test chains is shown. From the curves contained therein at constant J_i values of 25, 40, 50, 70 and 100 N/mm, the particular chain fracture stresses are assigned, see Figure 33. The upper bounding curve of this figure is characterised by the collapse failure which corresponds to the J_i value of 110 N/mm of the Type T chain. For the derivation of the requirement value, a stress of 400 N/mm^2 corresponding to twice the working load limit of Type T and Grade TH chains and a relative defect size of 0,2 was chosen. The choice of stress at double the Working Load Limit of 400 N/mm^2 was based on an impulsive loading factor of 2 which can arise in every hoisting device. The point with the coordinates (400 N/mm^2, a/d =0,2) shows a safety factor of 1,5 against collapse. If, as is usual, a safety factor relative to a defect size of 2 is assumed, then a relative permissible crack depth of 0,4 results. Hence, for the chain with a relative crack depth of 0,43 at a gross area nominal fracture stress of 400 N/mm^2, a J_i value of 70 N/mm is required. This requirement also emerges immediately from Figure 23 by plotting the dashed line, see Figure 34.

Thus the requirement point (A) in the diagram J = 70 N/mm and a/d = 0,43 is in contrast to the operational point (B) with J = 25 N/mm and a/d = 0,22. From this relationship the safety margins against collapse and defect depth given above result. Furthermore, relative to stress, a safety margin against crack initiation of 1,38 may still be derived. The requirement on the J integral value of 70 N/mm may be correlated with a notch impact energy on the basis of Figure 26. If one combines here the fracture stress of 400 N/mm^2 with the relative defect depth of 0,43, then the required notch impact energy of 30 J emerges, see Figure 35.

According to Figure 35, the requirement for the Grade VH chain at a fracture stress of 500 N/mm² which is twice the working load limit (250 N/mm²), would amount to 45 J. From Figure 34 this value correlates with a J integral value of 110 N/mm. Thus from Figure 33 a safety factor of 1,2 against crack initiation results. The collapse stress for the Grade VH chain in correspondence with the yield stress can be calculated to be proportionally high. On this basis, a safety factor against collapse of 1,35 results.

The required 30 J notch impact energy is met by the Type T chain at –40 °C. The Grade TH and VH chains with the determined notch impact energies of 9 to 14 J at –40 °C do not meet this requirement. Both these types of chains can reach 30 J notch impact energy in the region of 0 °C. These considerations correlate with the requirement that the lowest possible operating temperature be greater than or equal to the NDT temperature –20 K.

For Type T chain, this results in a temperature of –50 °C and thus the lowest permissible operating temperature is confirmed. As already noted, 0 °C as the lowest permissible operating temperature results from these requirements for Grade TH and VH chains.

13 Correlation of test results with data from the literature

From publications [6] regarding the correlation of J integral values with notch impact energy values, the scatterband in Figure 36 was taken, which also contains other well-known correlations such as Barsom-Rolfe. The IRSID correlation, which lies somewhat above this scatterband, is in very good agreement with the results of the present work and confirms the correlation of J_i = 70 N/mm with 30 J notch impact energy. An explanation for the position of the correlation curve above the scatterband lies in the high strength of the chain steels, which is still combined with considerable toughness.

14 Summary

High-strength, highly loaded, round steel chains must exhibit sufficient operational safety even under critical conditions as regards temperature and the effects of damage such as cracks. The material toughness has to be regarded as a decisive influential factor for operational safety. The objective of the present work was to investigate chains of various quality classes of different materials with different toughnesses and with defects of various depths at the lowest permissible operating temperature as to their load-bearing behaviour. These fracture mechanics considerations, underpinned by experiment, could be referred back to notch impact energy values which gave sufficient load-bearing capability for damaged chains. These notch impact energy values can be proven without difficulty in standard notch impact bend tests and thus be called upon for the standard requirements of minimum toughness of materials in the manufacture of round steel chains.

The investigations were performed on round steel chains of size 16 × 48 in conformance with ISO 3077. The chains dealt with here are a Type T chain in accordance with ISO 3077, a Grade TH chain in accordance with ISO 16877 and a Grade VH chain in accordance with ISO 16872. The Type T chain was made of a CrNiMo alloy steel while the Grade TH and VH chains were of manganese-boron steel.

For checking the load-bearing behaviour, chains with crack-like defects of depths relative to the diameter of 0,22, 0,43 and 0,64 were tested.

The evaluation of the results took place in accordance with brittle fracture and ductile fracture concepts with respect to the stress intensity factor, the J integral and CTOD value. These tests were performed on chain specimens as well as three-point bend specimens with spark-eroded slits and fatigue cracks.

From these tests, the transferability of the results from the specimens to the component chains could be confirmed.

In parallel with these tests, the material toughness was quantified in instrumented notch impact bend tests. In addition to the notch impact energy values, these tests also supplied the brittle-ductile transition temperature relevant to the particular material. The determined results gave the following requirements for the lowest permissible operating temperature (T_{min}) and notch impact energy (KV) for operational safety behaviour of round steel chains as regards their load-carrying capacity in the cracked condition and brittle-ductile transition temperature for the individual chains investigated:

— Type T T_{min} = –40 °C, KV (–40 °C) $\geqslant$ 30 J

— Grade TH T_{min} = 0 °C, KV (0 °C $\geqslant$ 30 J

— Grade VH T_{min} = 0 °C, KV (0 °C) $\geqslant$ 45 J

Assuming a maximum permissible relative defect size of 0,22 and a failure stress of a minimum of twice the working stress, then, from the determined results safety factors of 1,5 against collapse and 2 on crack size result. These factors are valid for the Type T and Grade TH chains. Thus, they conform to the usual requirements. The correlations between the notch impact energy KV and the J integral values emerging from the determined results lie in the upper region of the correlations published in the literature.

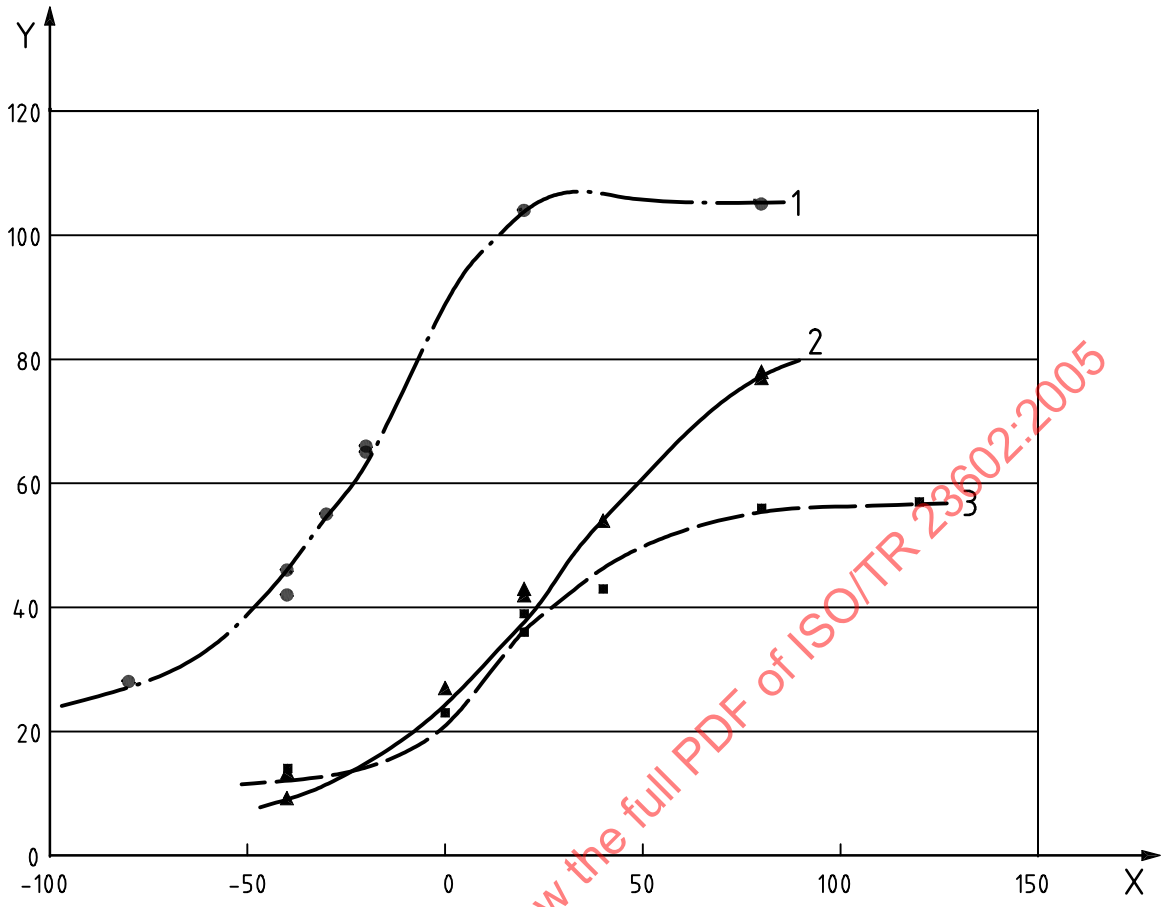

Key

X temperature, T, °C
Y C_V, toughness, J

1 type T
2 grade TH
3 grade VH

Figure 1 — Results C_V tests: Standard specimen (EN 10045)

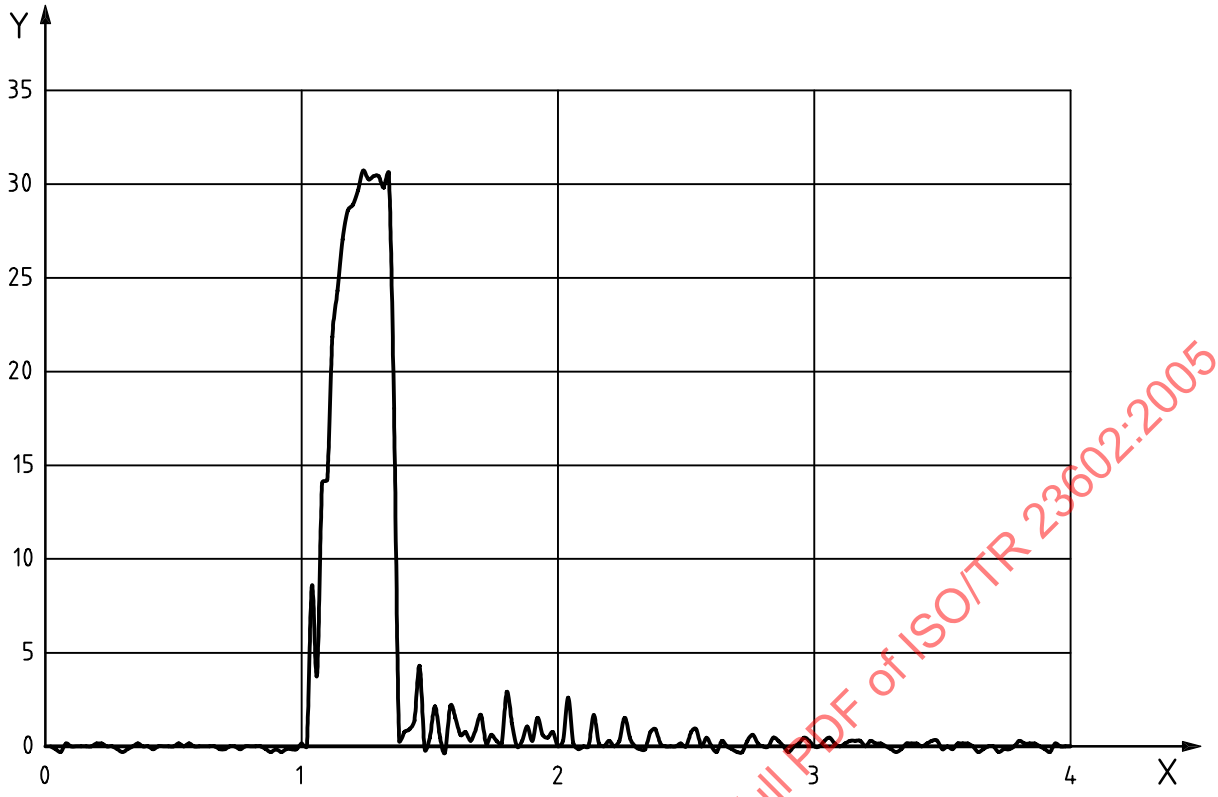

a) Test material Type T, temperature = –40 °C

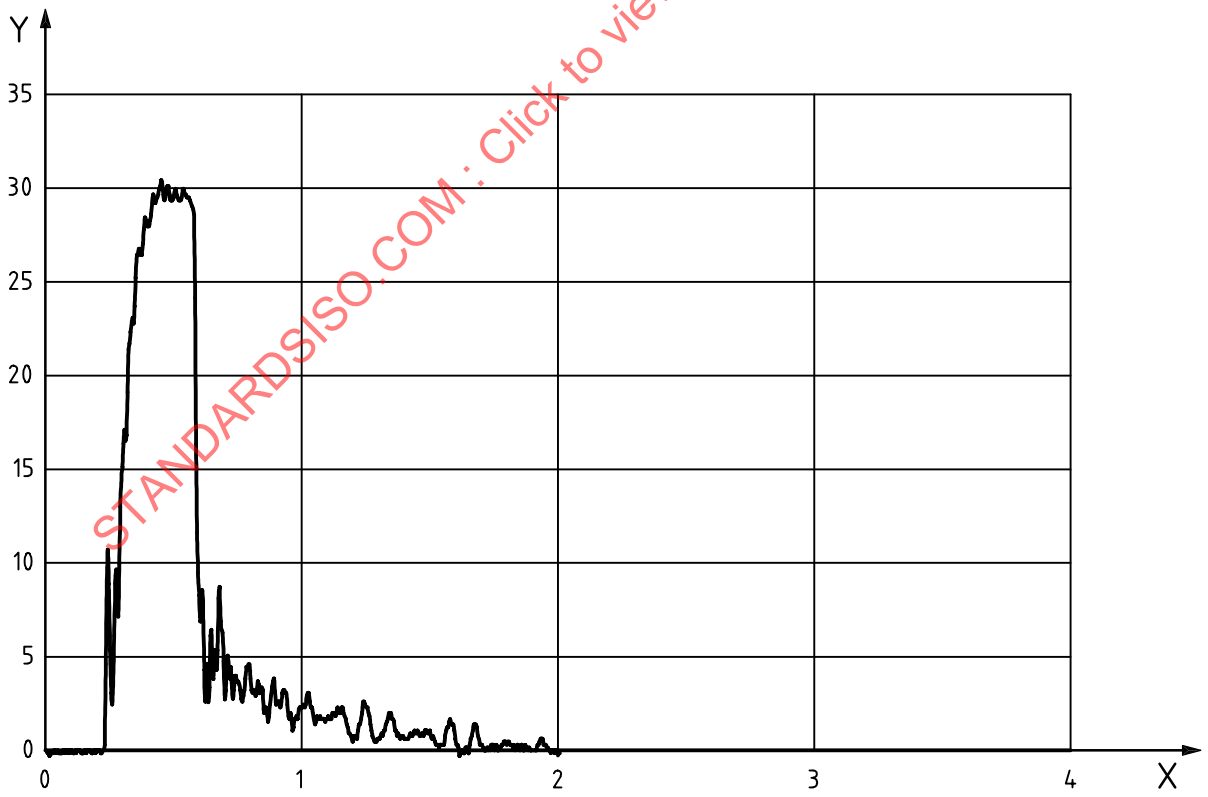

b) Test material Type T, temperature = –30 °C

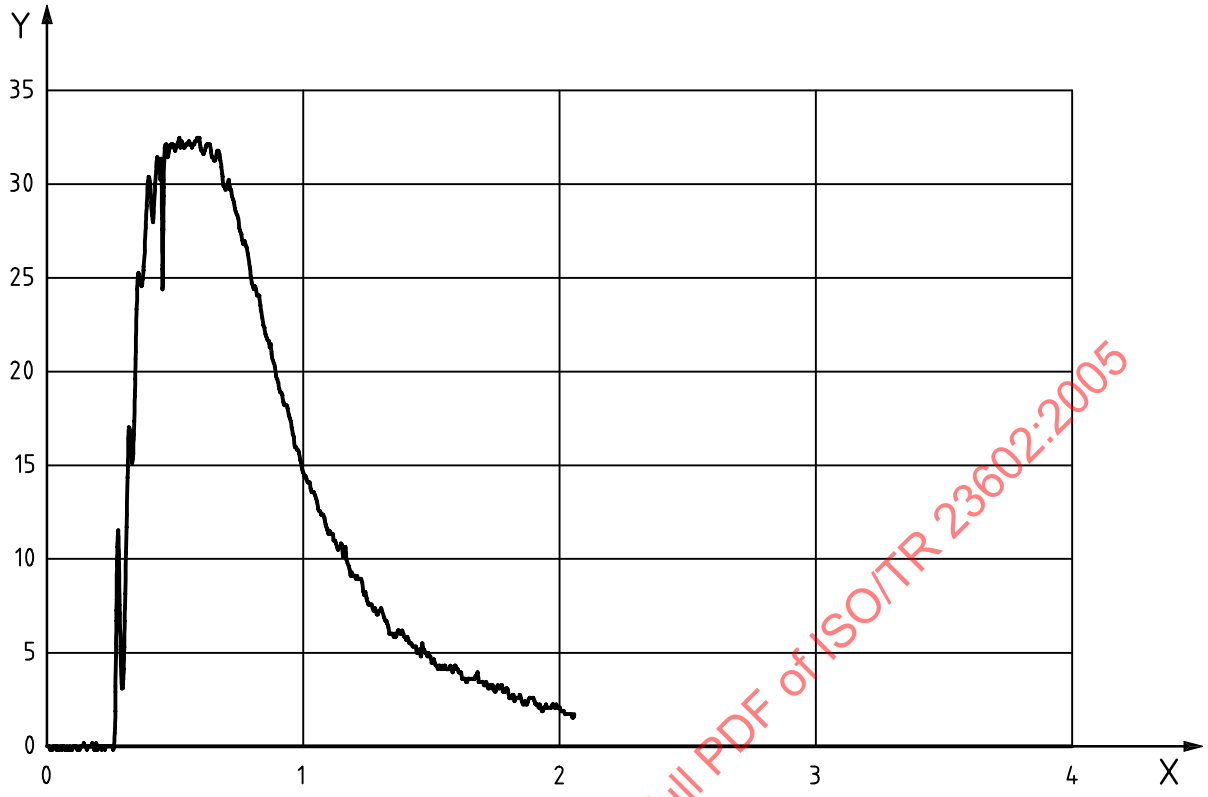

c) Test material Type T, temperature = +20 °C

Key

X time, t, ms
Y load, kN

Figure 2 — Load-time diagram for instrumented C_V

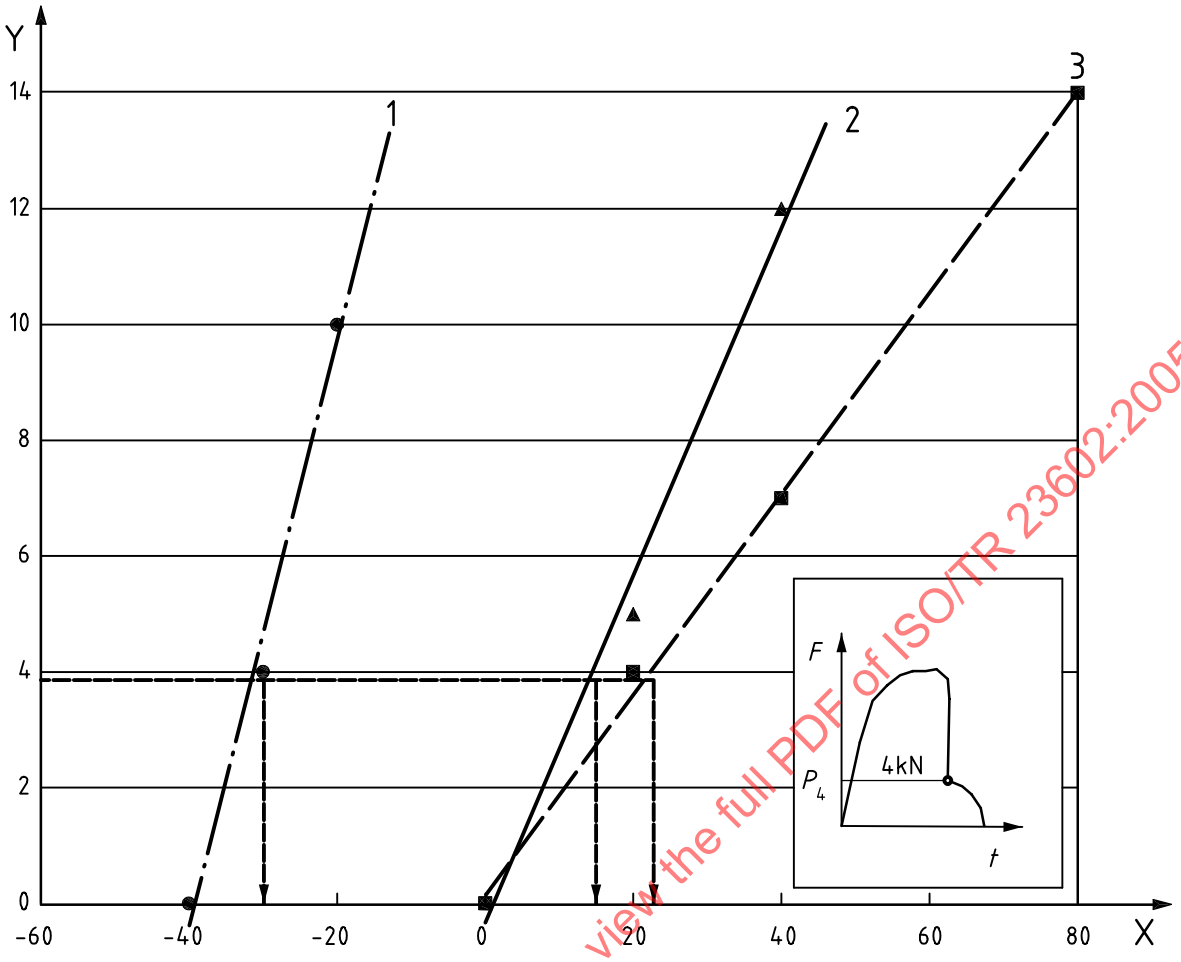

Key

X test temperature, T, °C
Y crack arrest load, F_{p4}, kN

1 type T
2 grade TH
3 grade VH

Figure 3 — Crack arrest load as function of temperature

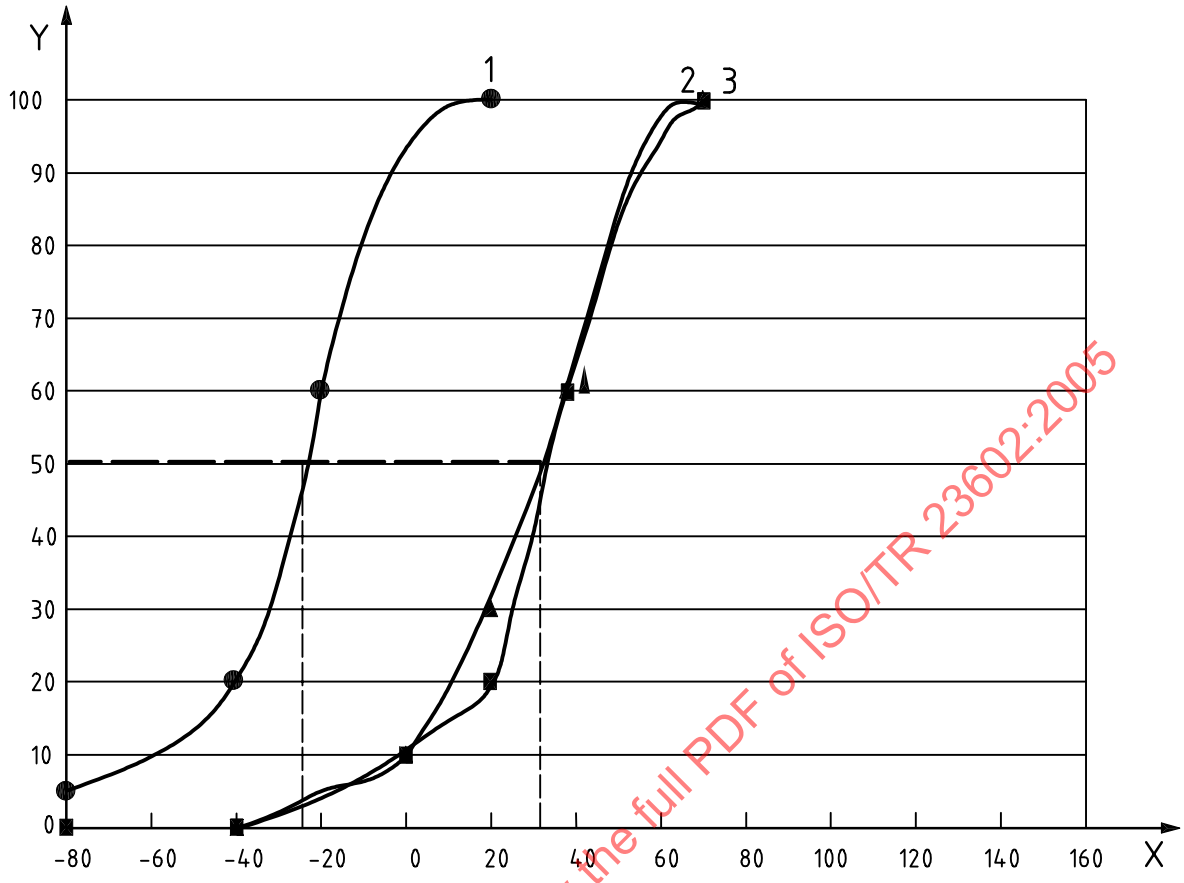

Key

X test temperature, T, °C
Y noncrystalline area, %

1 type T
2 grade TH
3 grade VH

Figure 4 — Noncrystalline area in C_V — Test

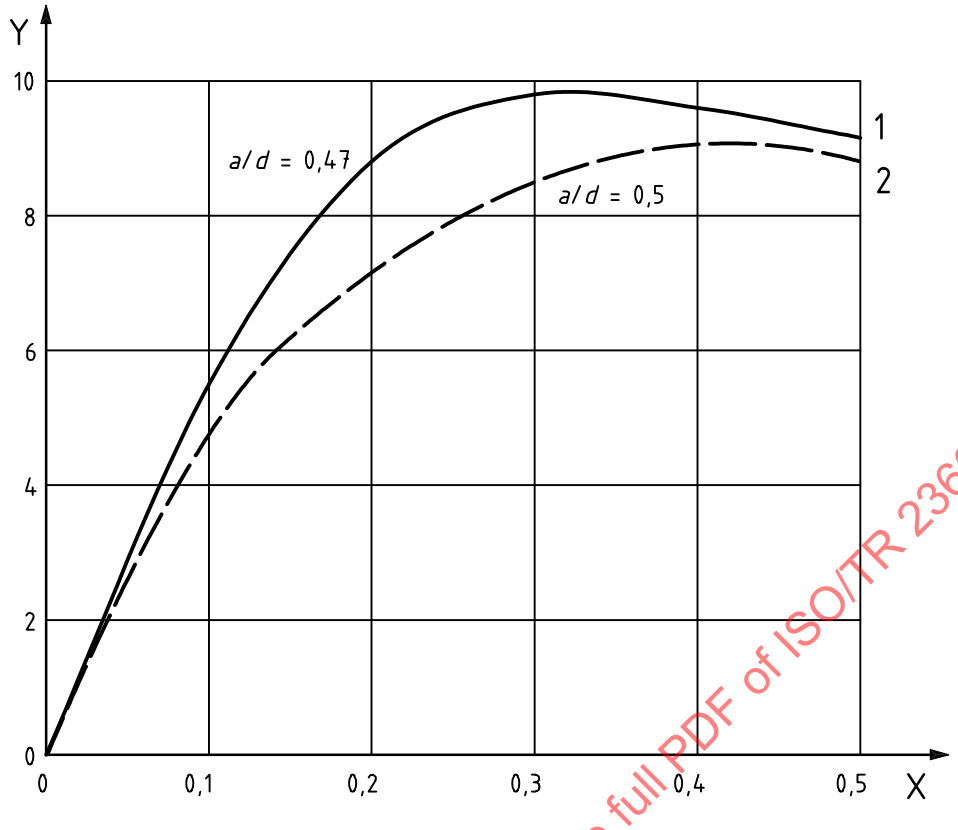

Key

X COD, [mm]
Y load, F, kN

1 fatigue crack
2 eroded slit

Figure 5 — Load–COD diagram for TPB specimens with fatigue crack and eroded slits material type T, T = –40 °C

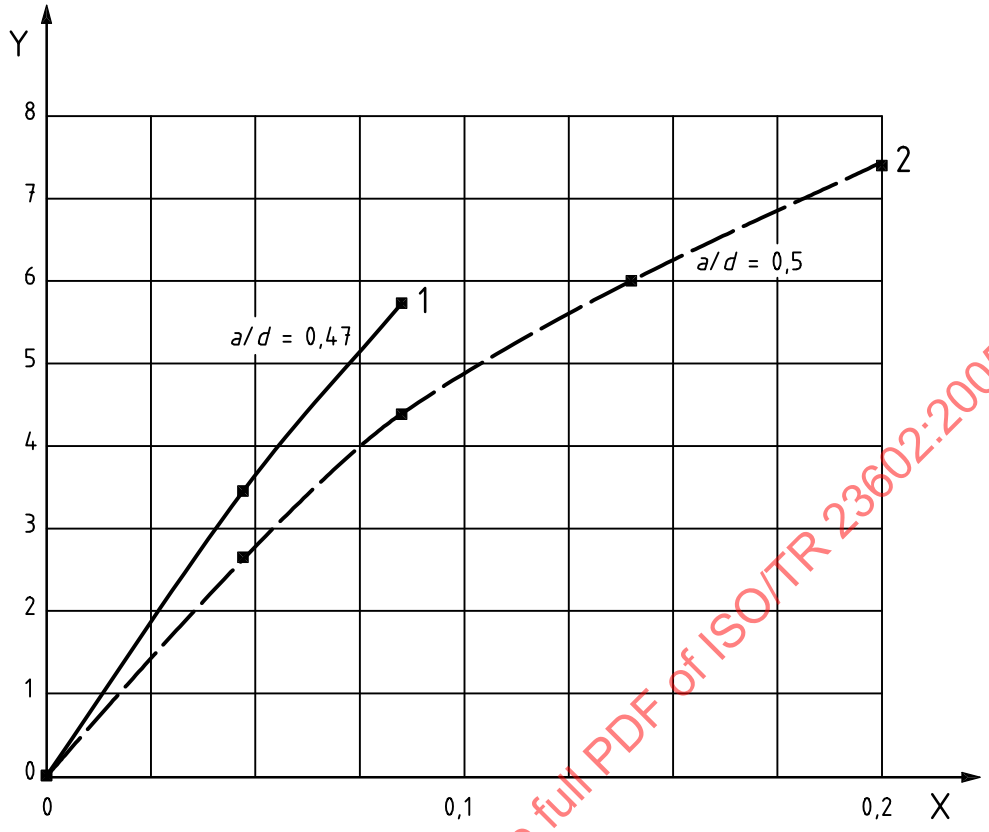

Key

X COD, mm
Y load, F, kN

1 fatigue crack
2 eroded slit

Figure 6 — Load–COD diagram for TPB specimens with fatigue crack and eroded slits material grade VH, T = –40 °C

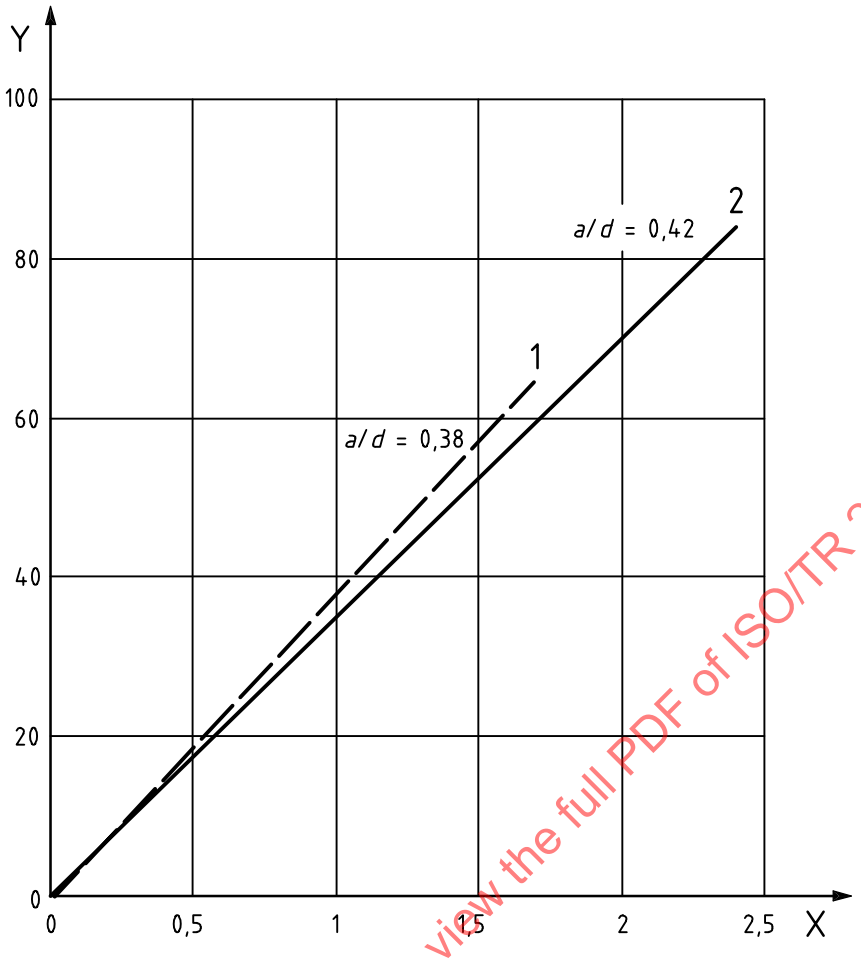

Key

X displacement, Δ, mm
Y load, F, kN

1 pre-cracked
2 eroded slit

Figure 7 — Comparison of pre-cracked and eroded chain link material grade VH, T = –40 °C

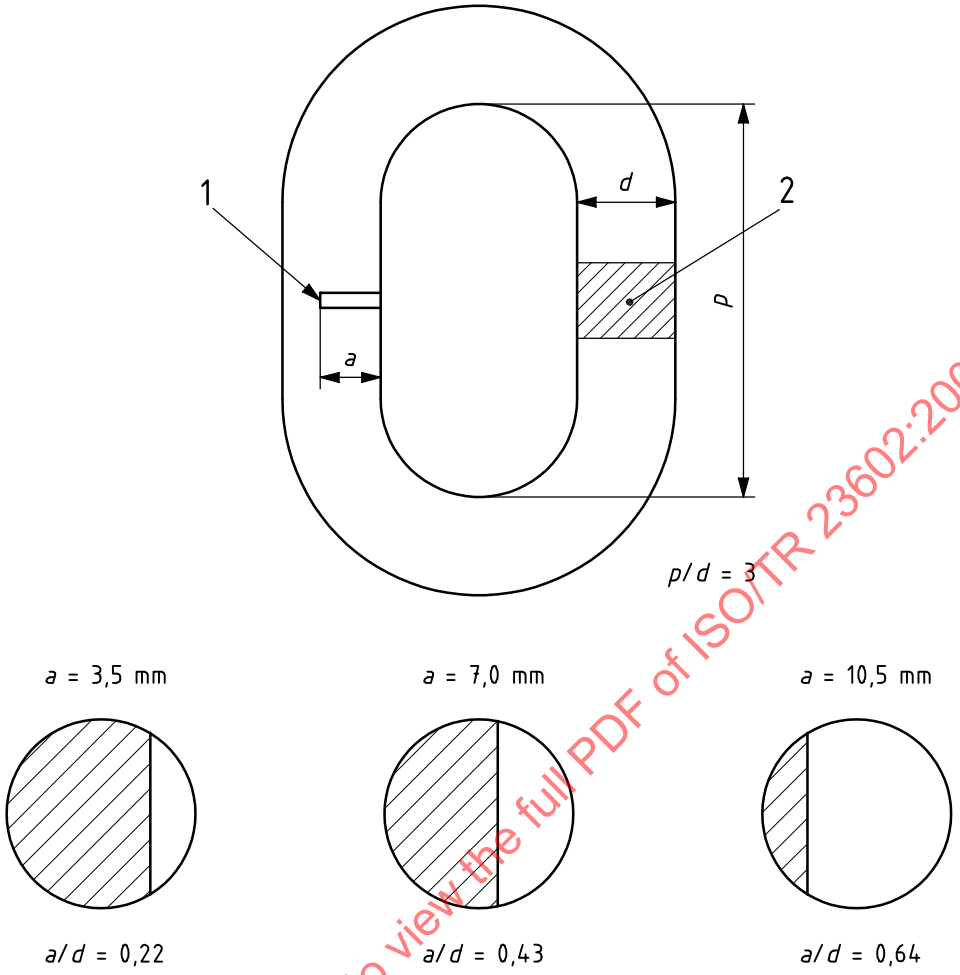

Key

1 eroded slit

2 weld

Figure 8 —Chain link specimen

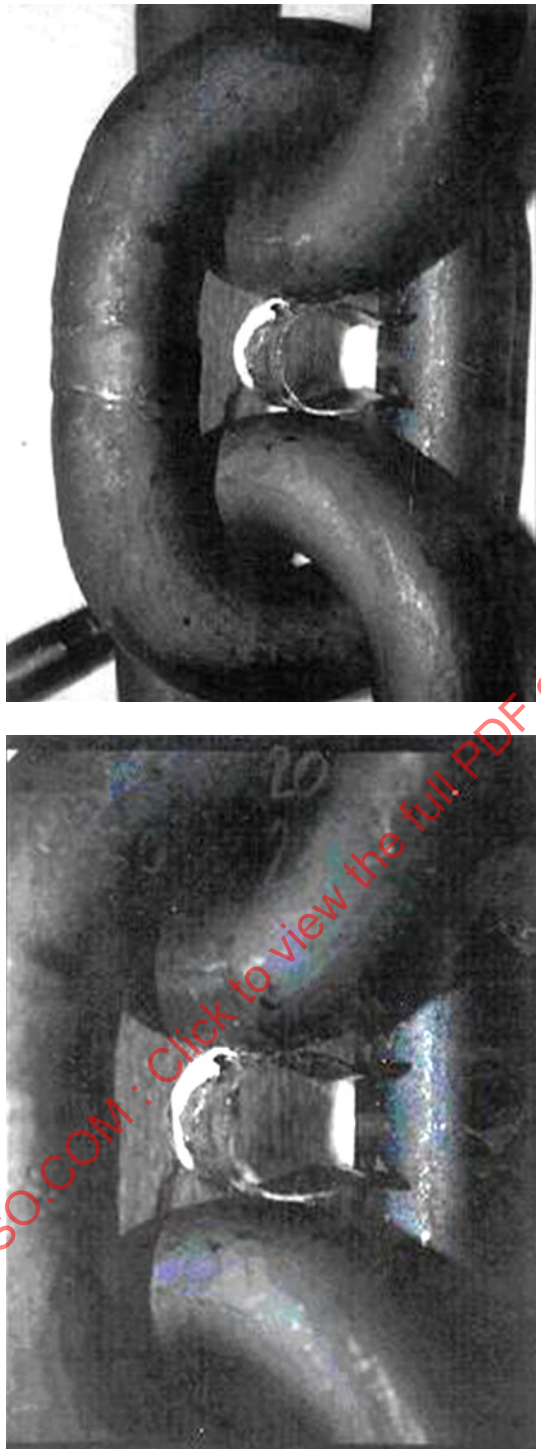

Figure 9 — Clip gauge fixed in chain link

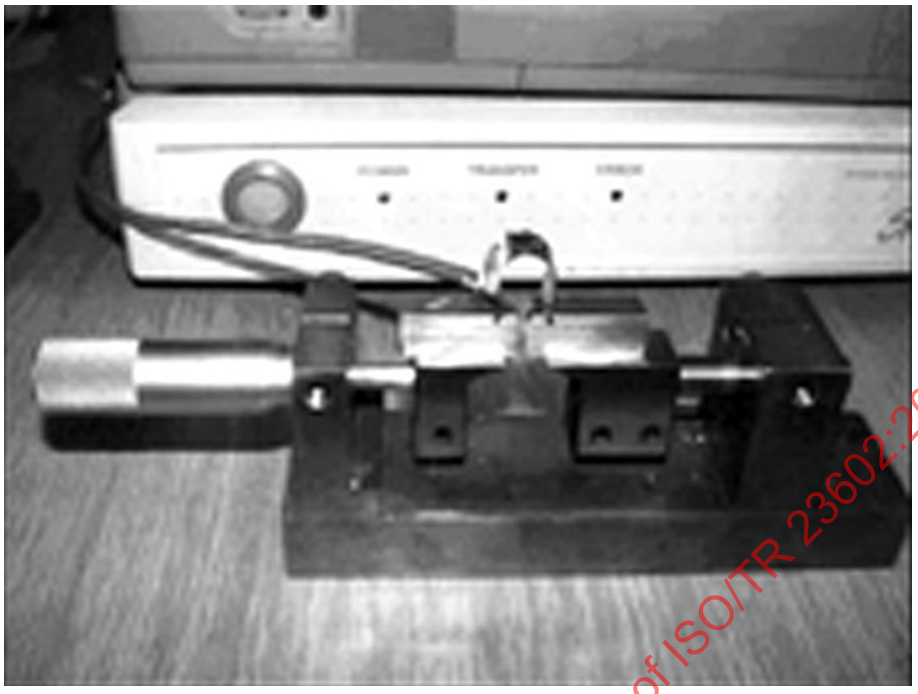

Figure 10 — Calibration of clip gauge for COD measurement

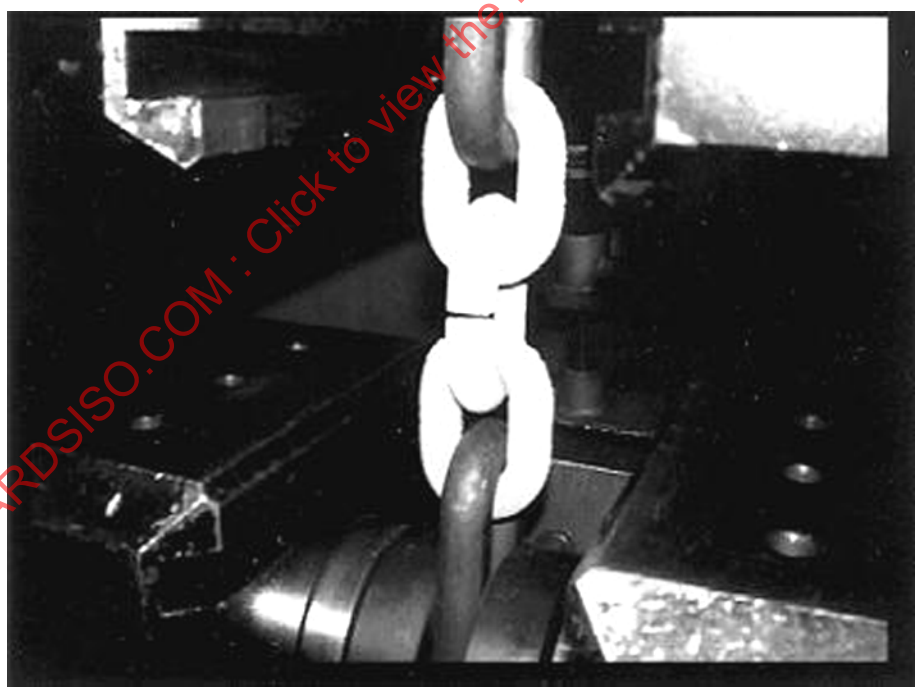

Figure 11 — Test specimen at –40 °C**, three links**

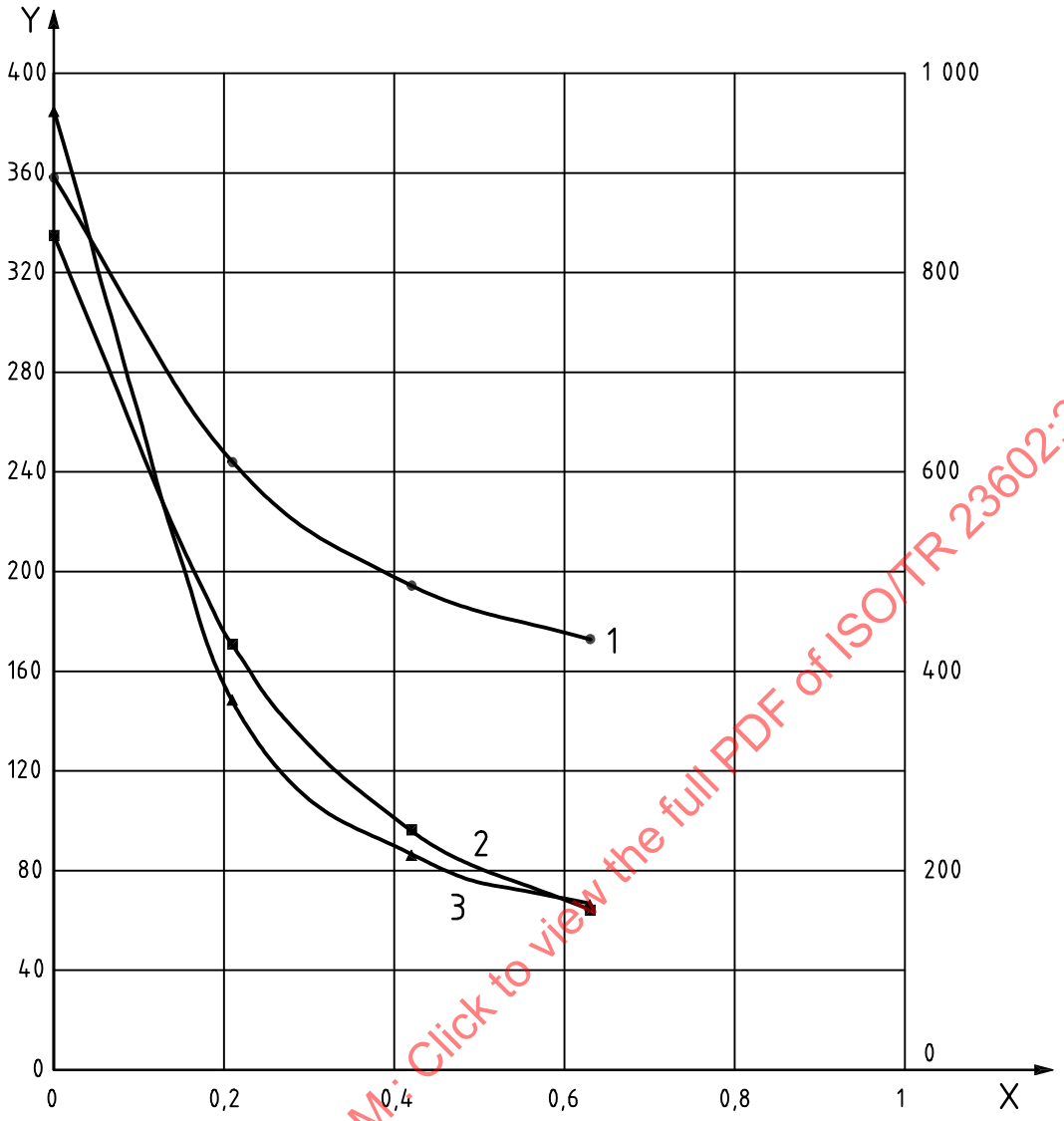

Key

X relative slit size, a/d
Y left: maximum load, F_{max}, kN
Y right: nominal remote tensile stress, σ_{n0}, MPa

1 type T
2 grade TH
3 grade VH

Figure 12 — Effect of slit size on loadability of chain, T = –40 °C

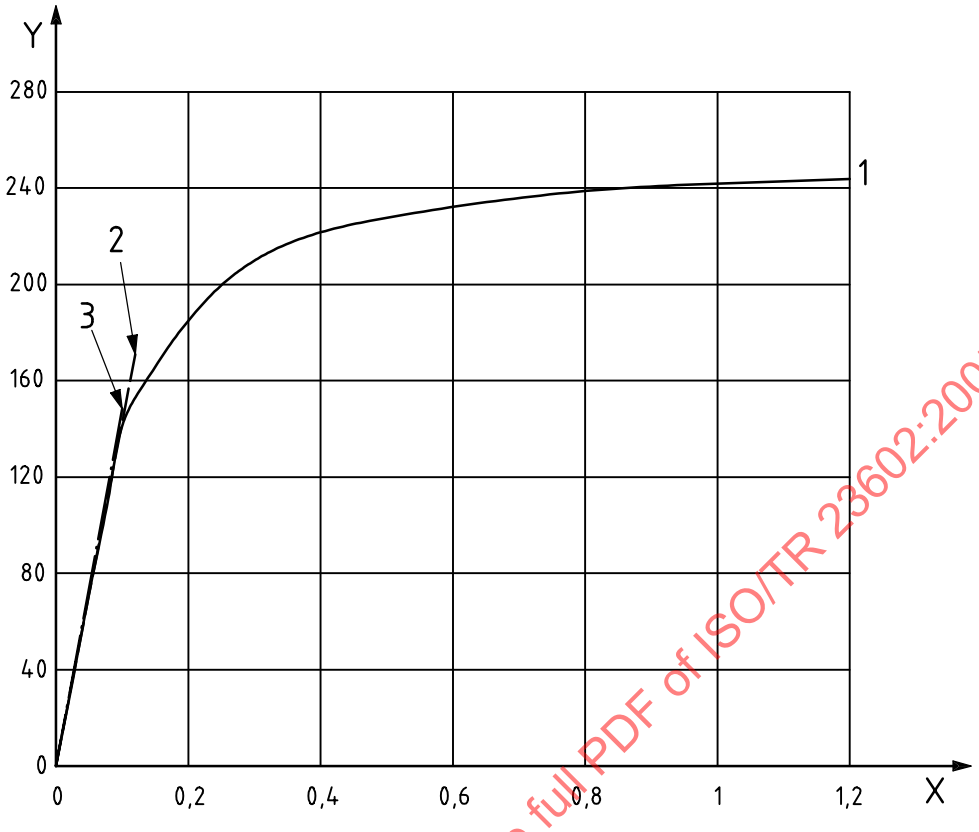

Key

X COD, mm
Y load, F, kN

1 type T
2 grade TH
3 grade VH

Figure 13 — Load–COD diagram for tension tests on chains with eroded slit, T = –40 °C, a/d = 0,22

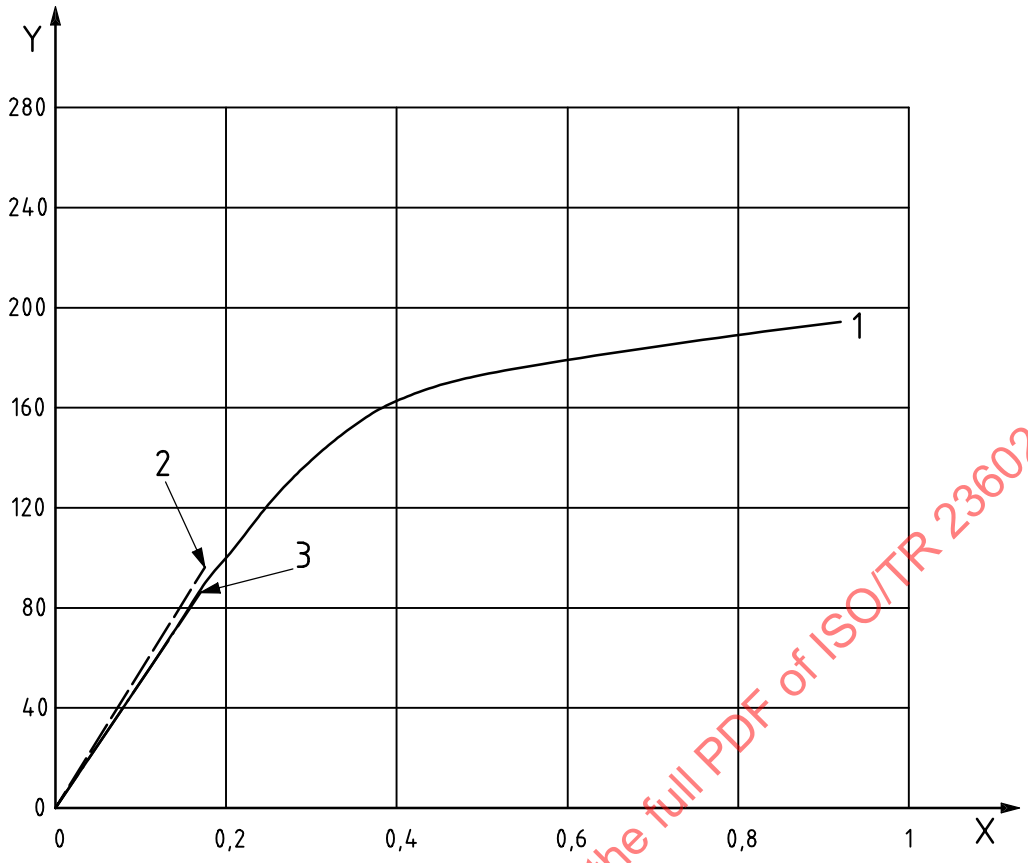

Key

X COD, mm
Y load, F, kN

1 type T
2 grade TH
3 grade VH

Figure 14 — Load–COD diagram for tension tests on chains with eroded slit, T = –40 °C, a/d = 0,43

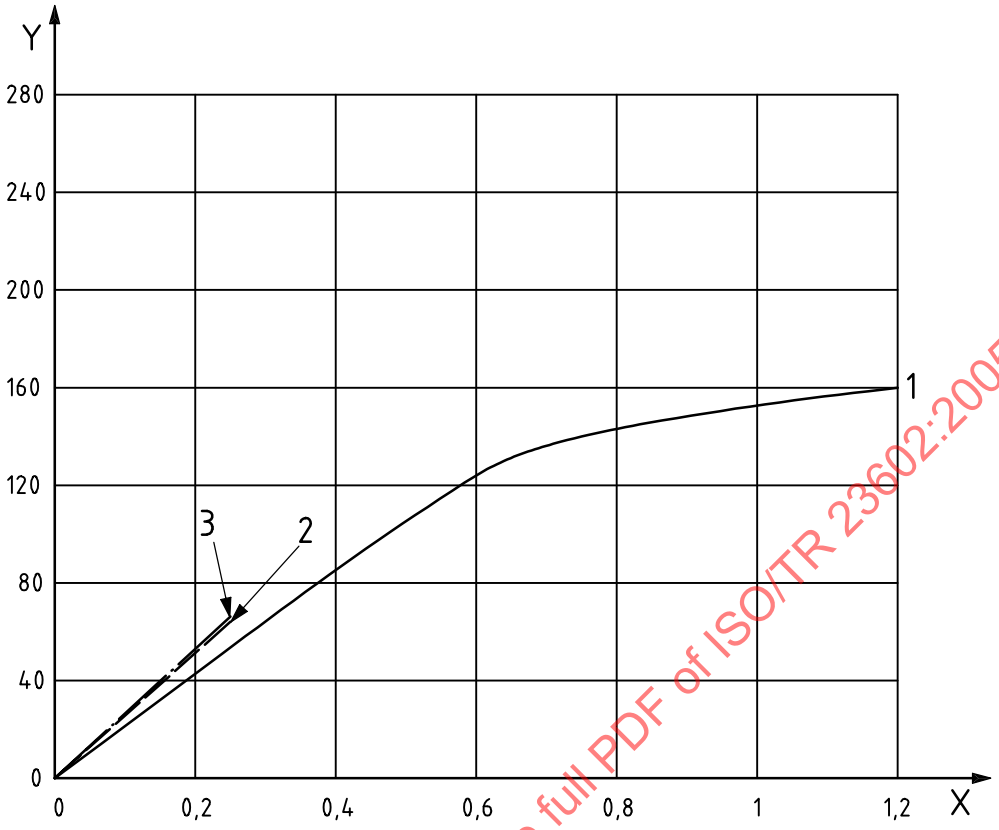

Key

X COD, mm
Y load, F, kN

1 type T
2 grade TH
3 grade VH

Figure 15 — Load–COD diagram for tension tests on chains with eroded slit, T = –40 °C, a/d = 0,64

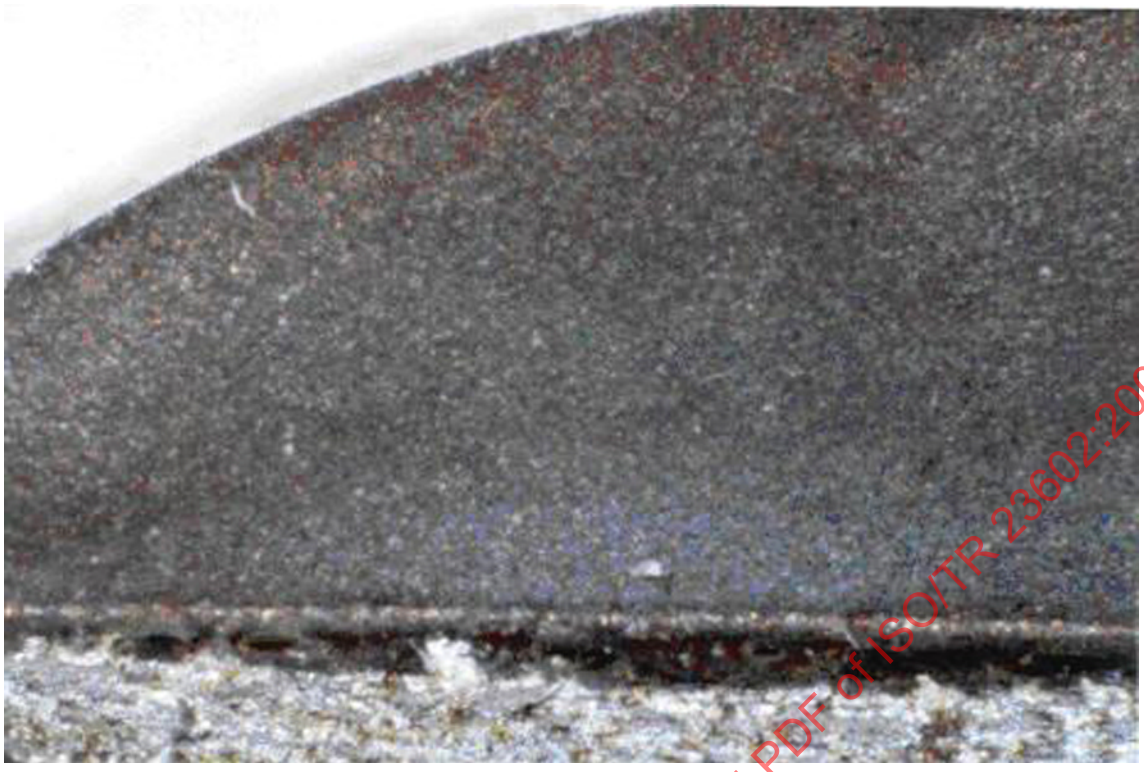

Figure 16 — Stable crack growth chain Type T, a/d = 0,22 — Marked by heat tinting

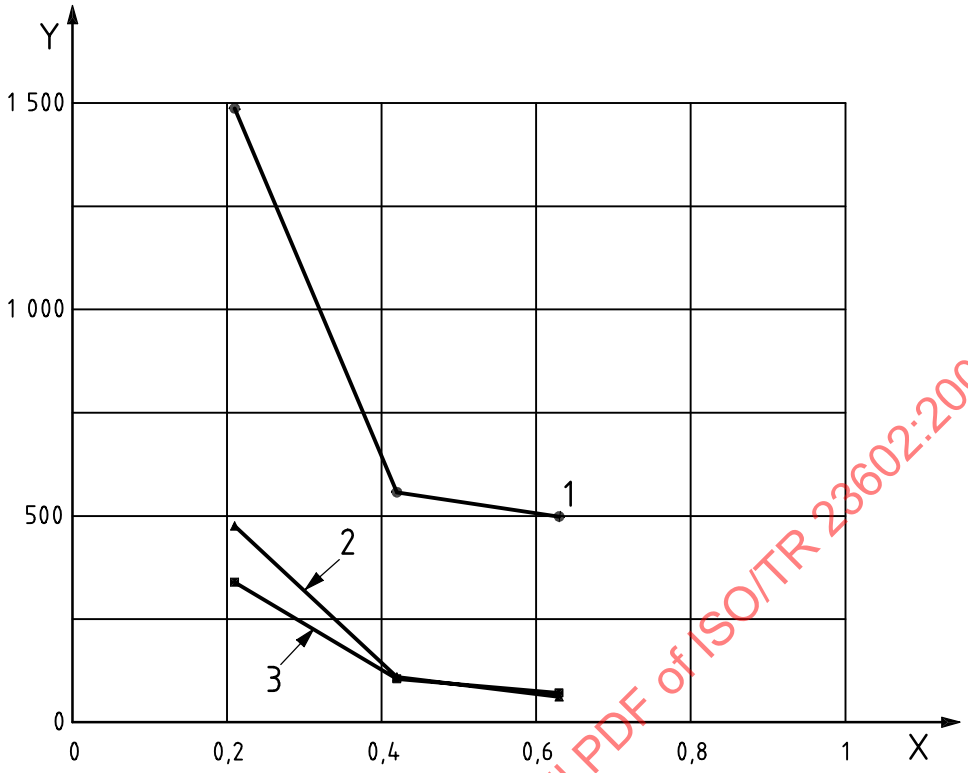

Key

X slit size, a/d

Y absorbed energy, U_{max}, J

1 type T

2 grade TH

3 grade VH

Figure 17 — Effect of slit size on absorbed energy of chains, T = –40 °C

Dimensions in millimetres

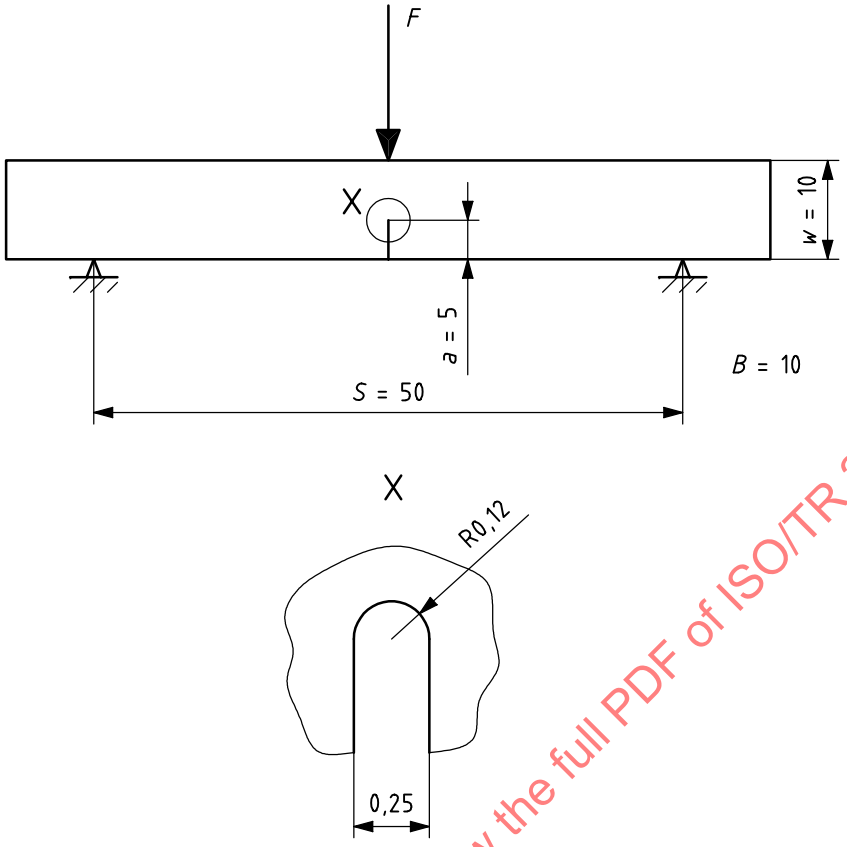

Figure 18 — Fracture mechanics tests on TPB specimens

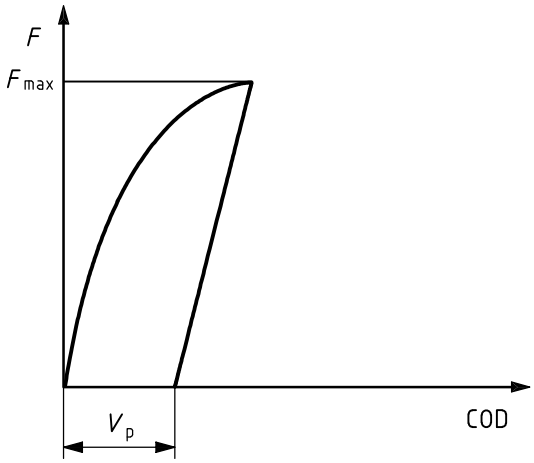

a) COD concepts

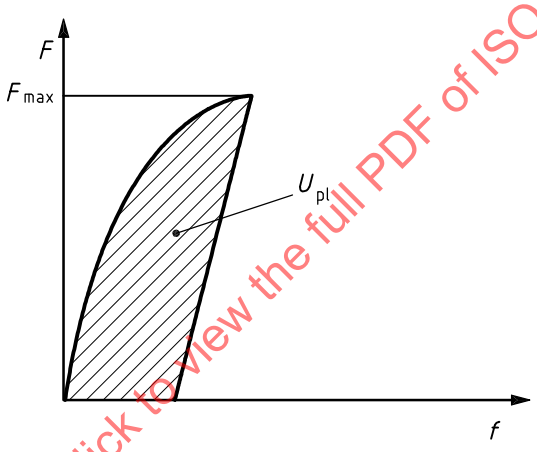

b) J-Integral concepts

Figure 19 — Fracture mechanics concepts

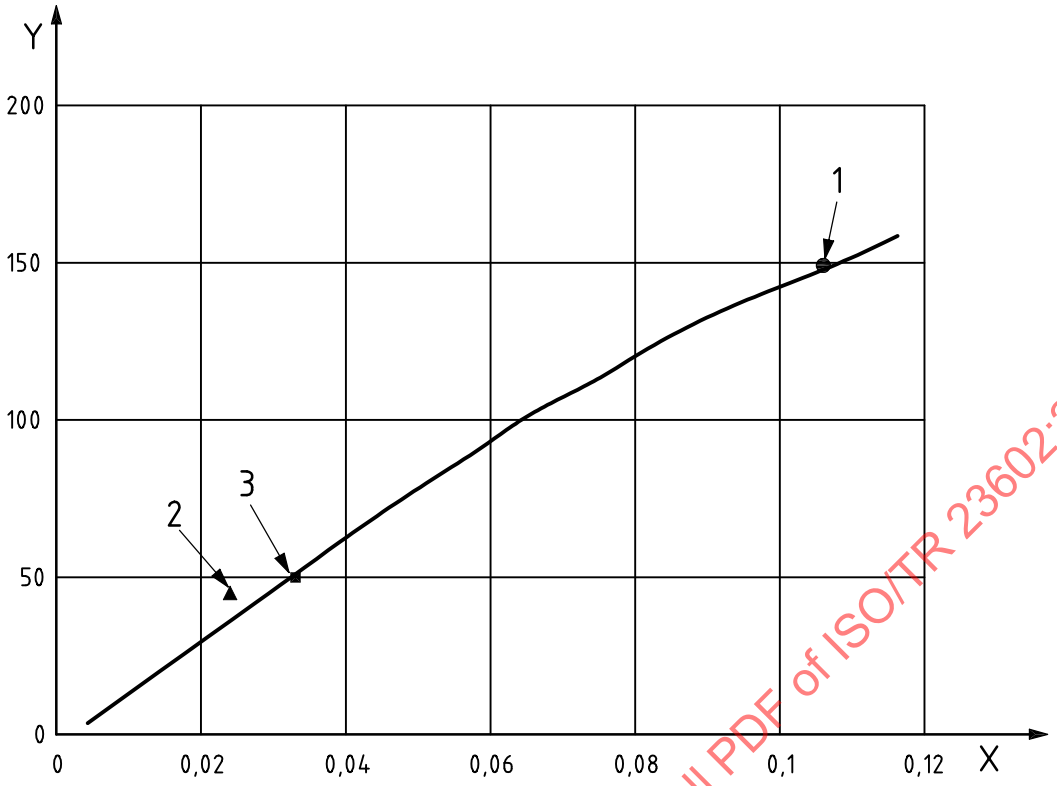

Key

X crack tip opening displacement, δ_{tot}, mm
Y J integral, J_{tot}, N/mm

1 type T
2 grade TH
3 grade VH

Figure 20 — Fracture toughness values for TPB specimens with eroded slits, T = –40 °C, a/w = 0,5

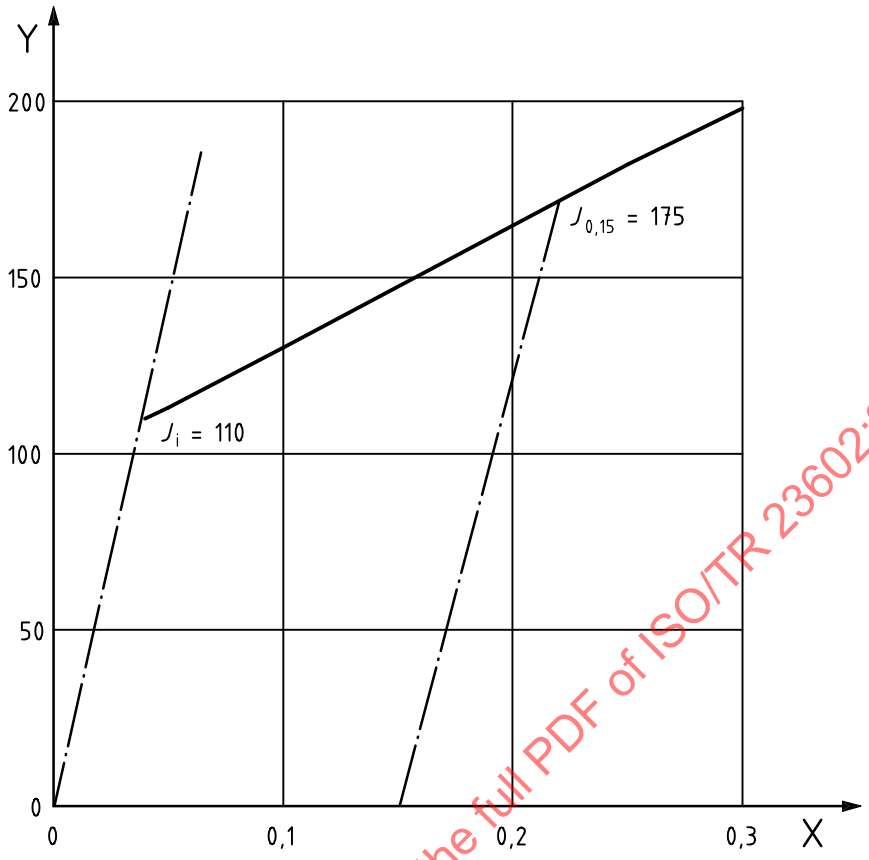

Key

X crack opening, Δa, mm

Y J integral, J, N/mm

Figure 21 — R-curves material Type T, T = –40 °C, a/w = 0,4

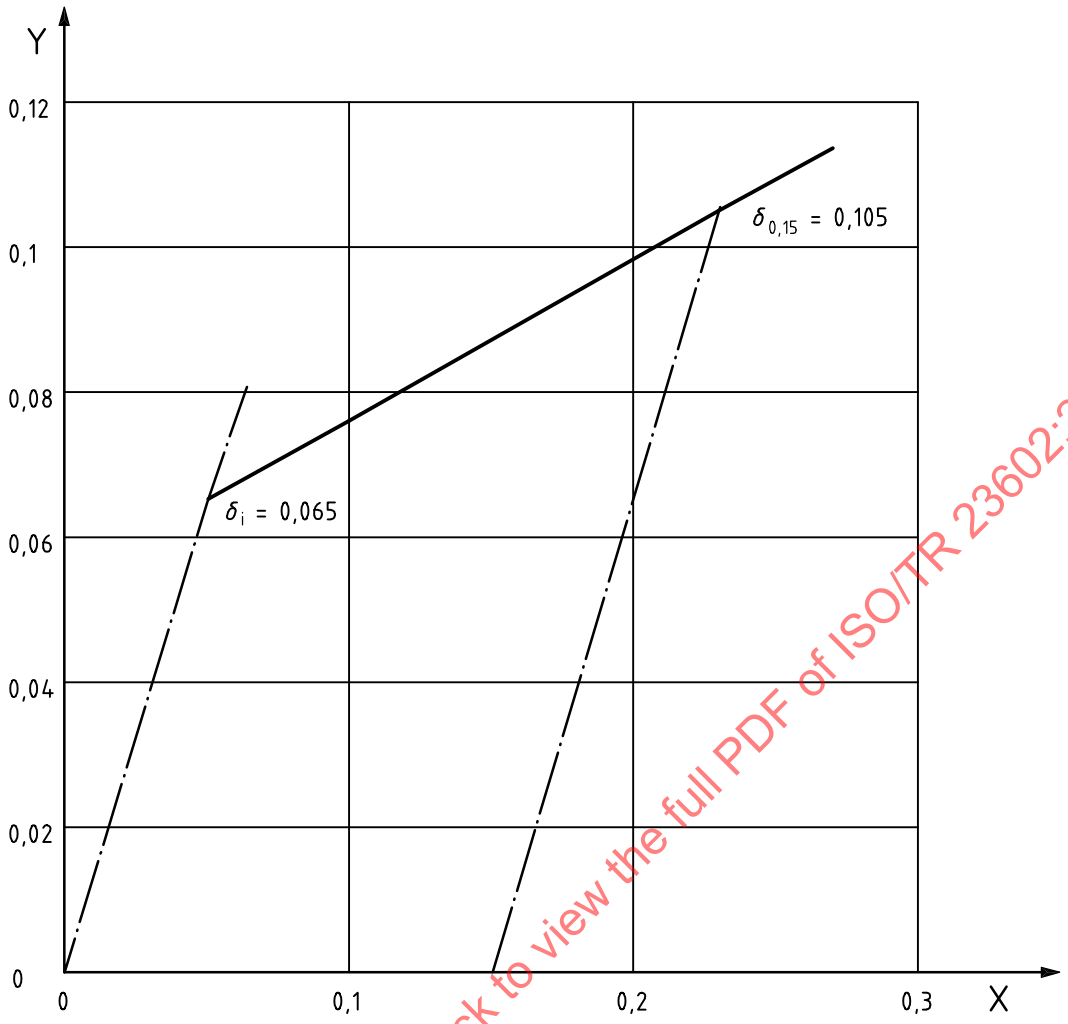

Key

X crack opening, Δa, mm

Y CTOD, mm

Figure 22 — R-curves material Type T, T = –40 °C, a/w = 0,4

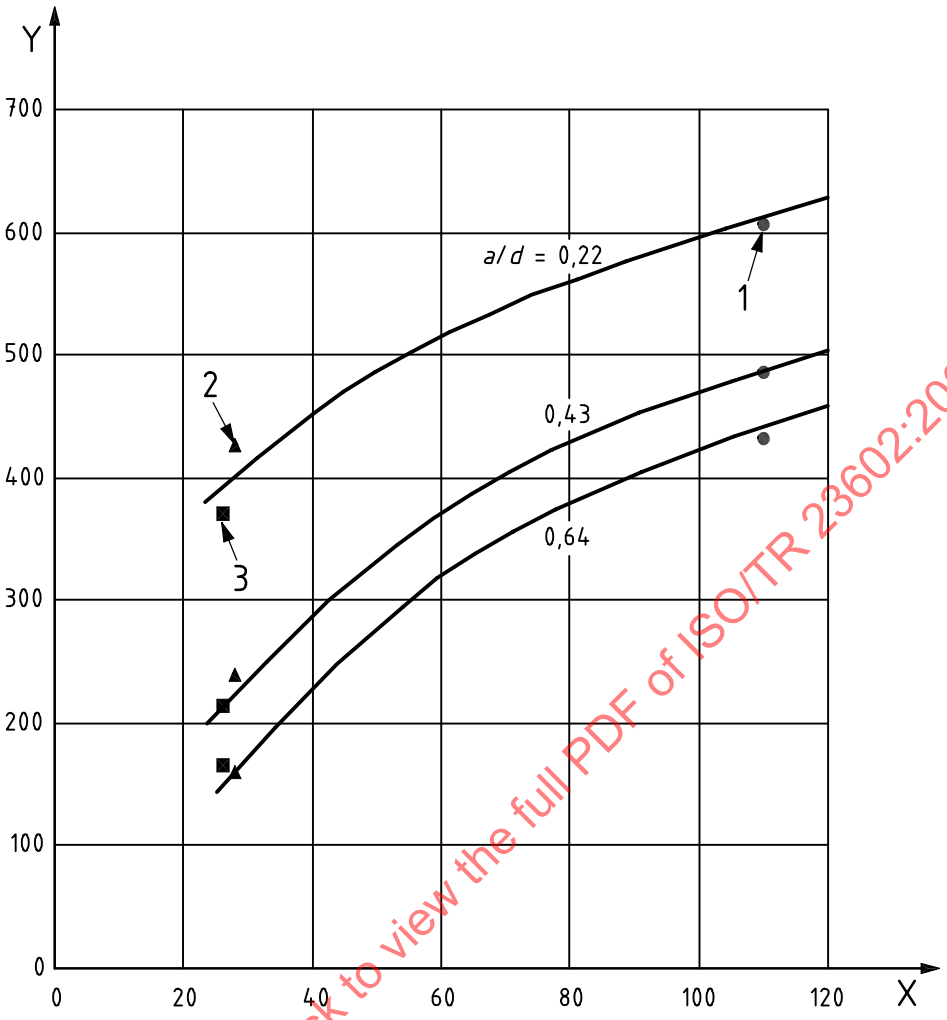

Key

X J integral, J_i, N/mm
Y remote tensile stress, σ_{n0}, MPa
1 type T
2 grade TH
3 grade VH

Figure 23 — Nominal fracture stress in chain link, correlated with fracture mechanics properties

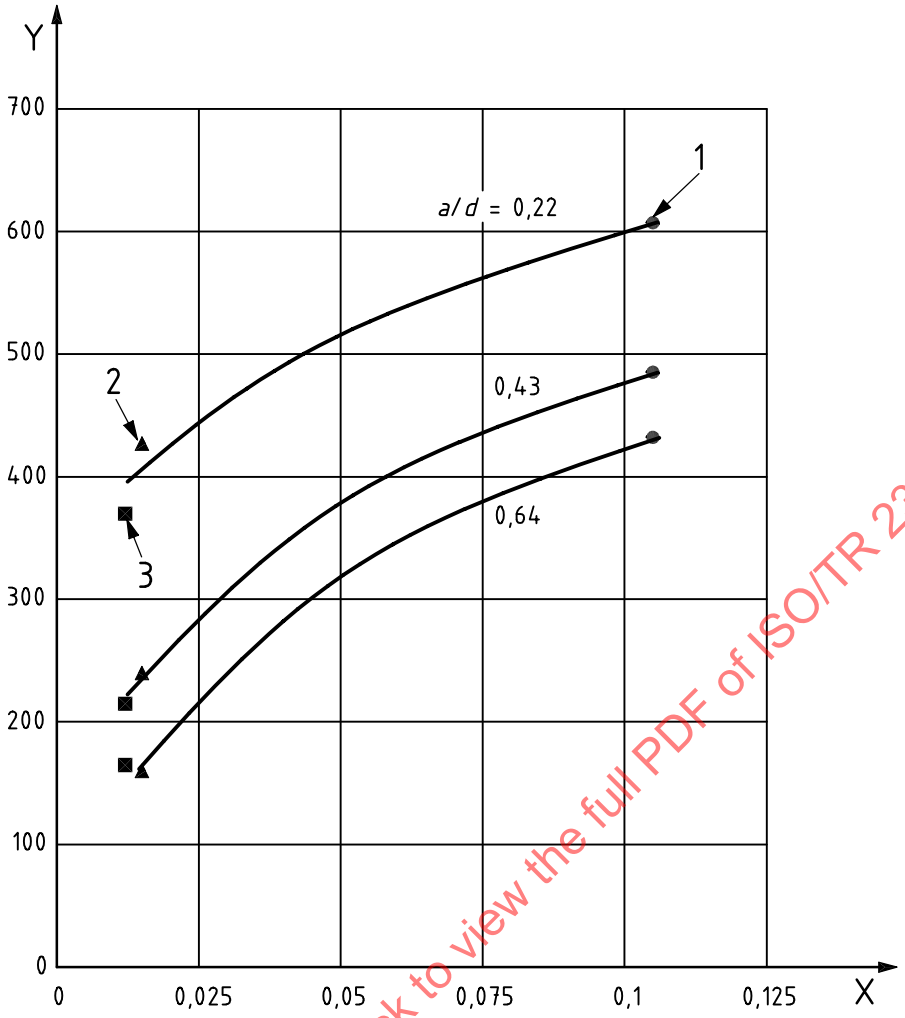

Key

X CTOD, mm

Y remote tensile stress, σ_{n0}, MPa

1 type T

2 grade TH

3 grade VH

Figure 24 — Nominal fracture stress in chain link correlated with fracture mechanics properties

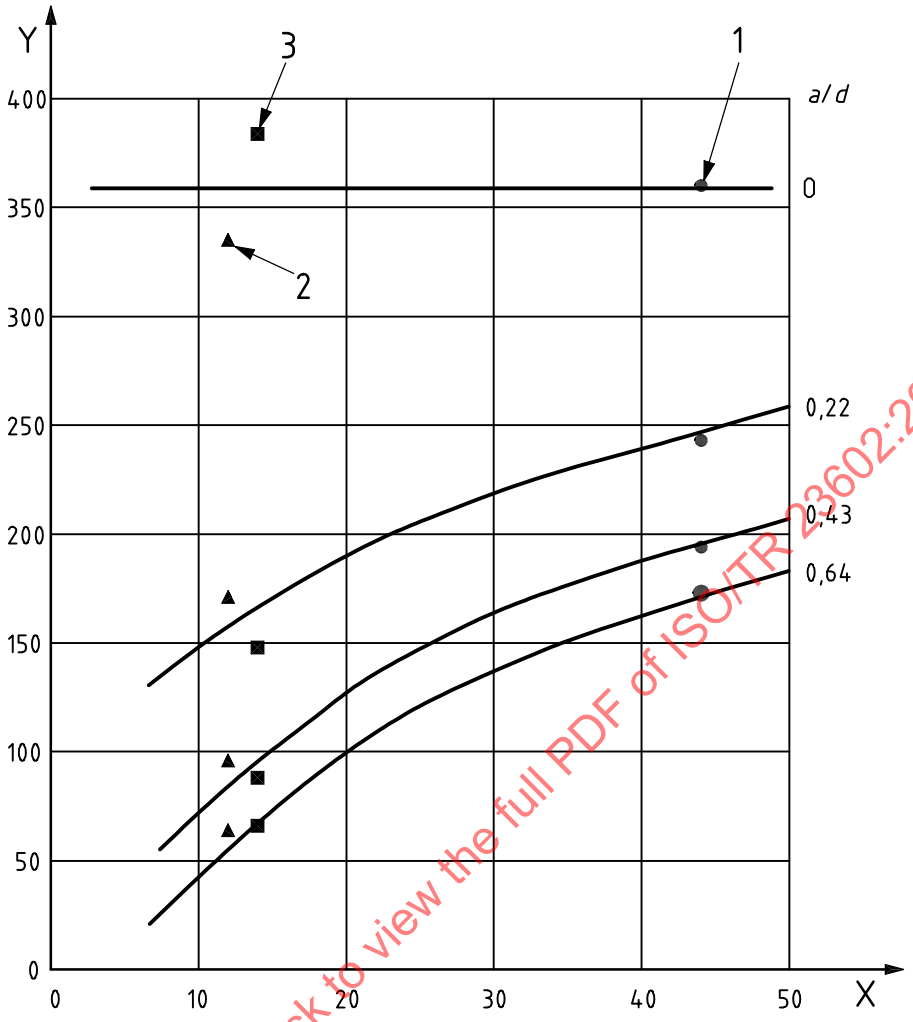

Key

X C_v toughness, J
Y fracture load, F_{max}, kN

1 type T
2 grade TH
3 grade VH

Figure 25 — Correlation of fracture load and C_v toughness

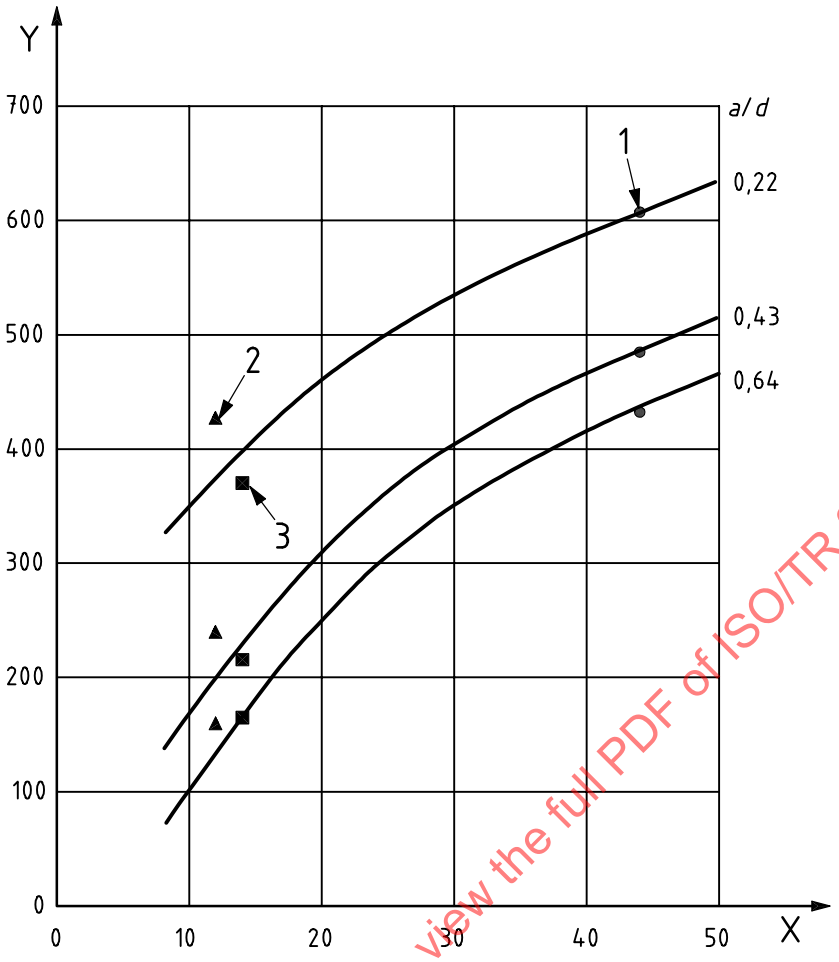

Key

X C_v toughness, J
Y nominal remote tensile stress, σ_{n0}, MPa

1 type T
2 grade TH
3 grade VH

Figure 26 — Correlation nominal fracture stress of chain and C_v toughness

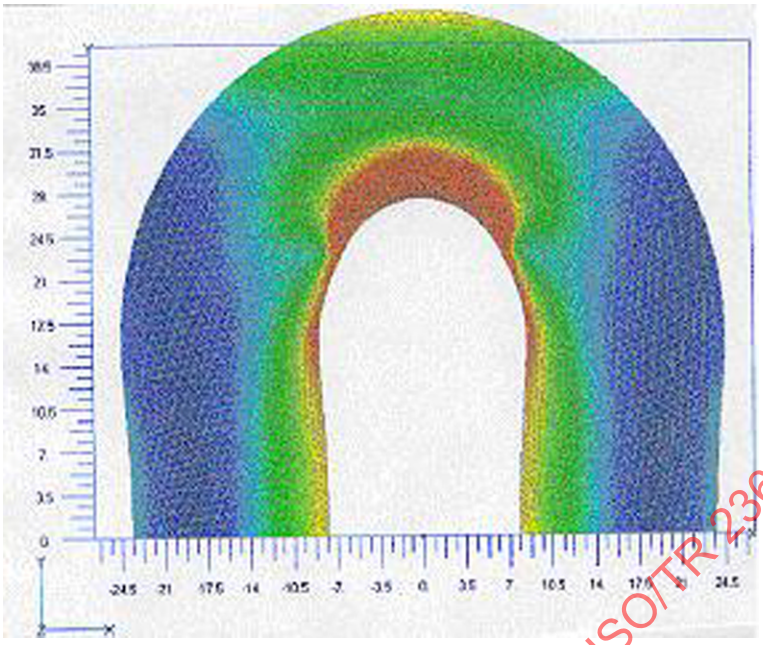

Figure 27 — Finite element analysis of chain links with eroded slit, a/d = 0

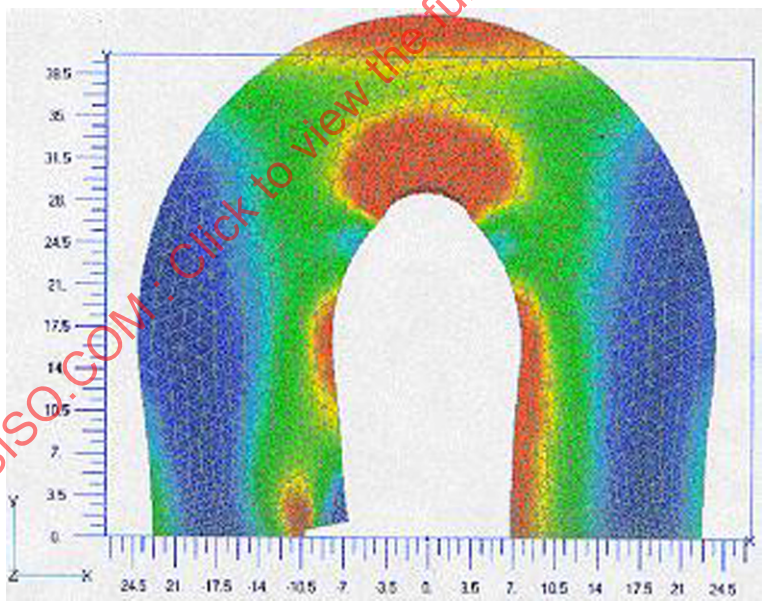

Figure 28 — Finite element analysis of chain links with eroded slit, a/d = 0,22

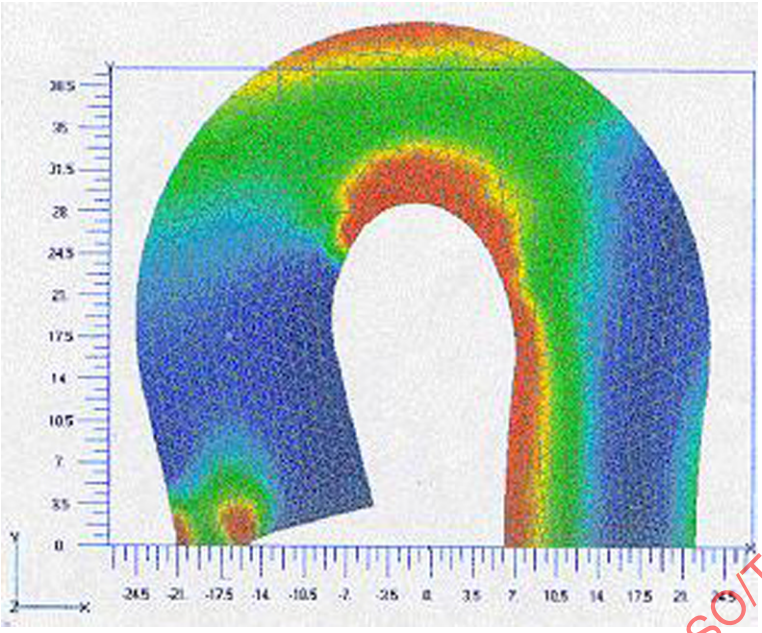

Figure 29 — Finite element analysis of chain links with eroded slit, a/d = 0,64

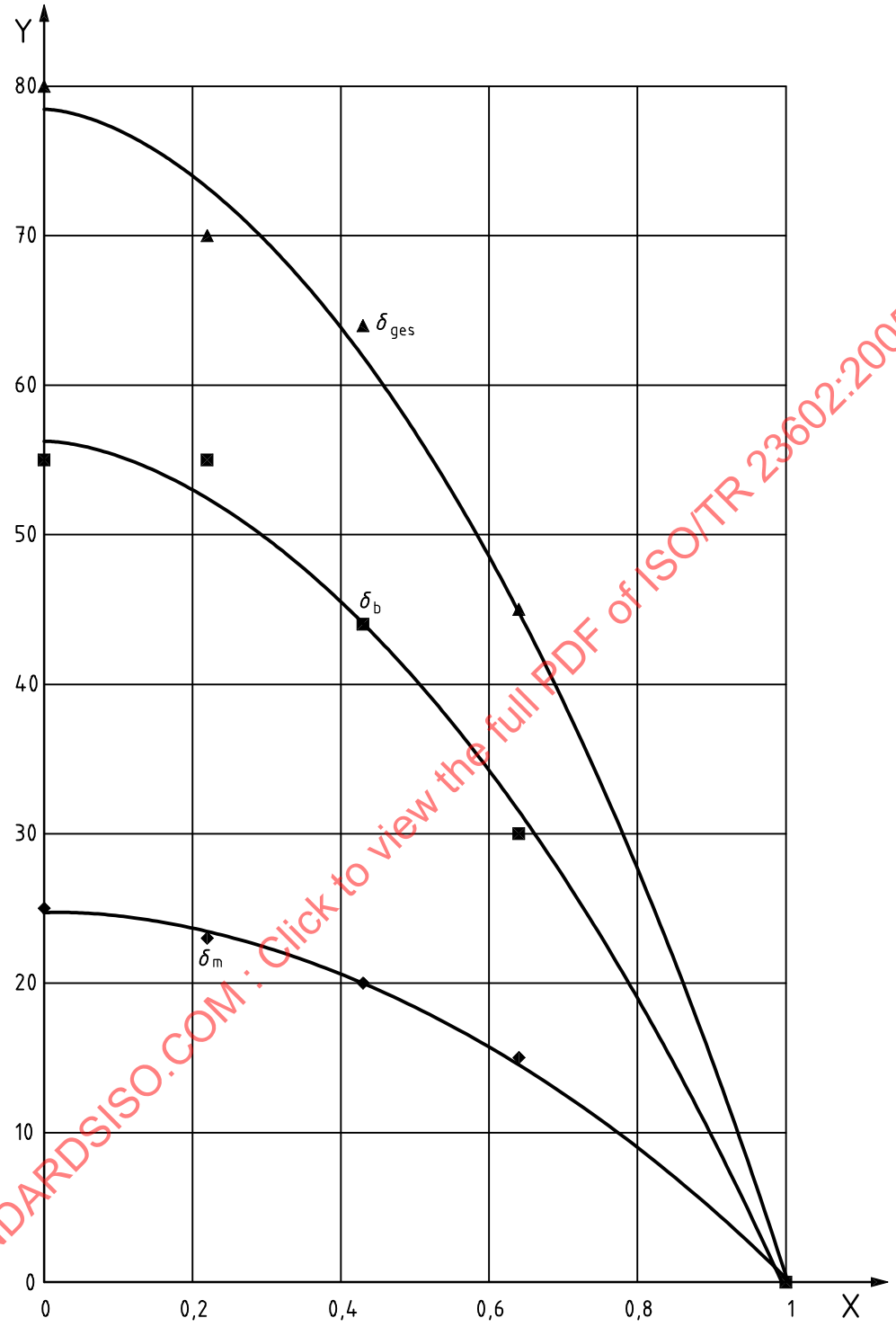

Key

X relative crack depth, *ald*

Y remote nominal tensile stress, σ_{n0}, MPa

Figure 30 — Nominal stresses in cracked chain link

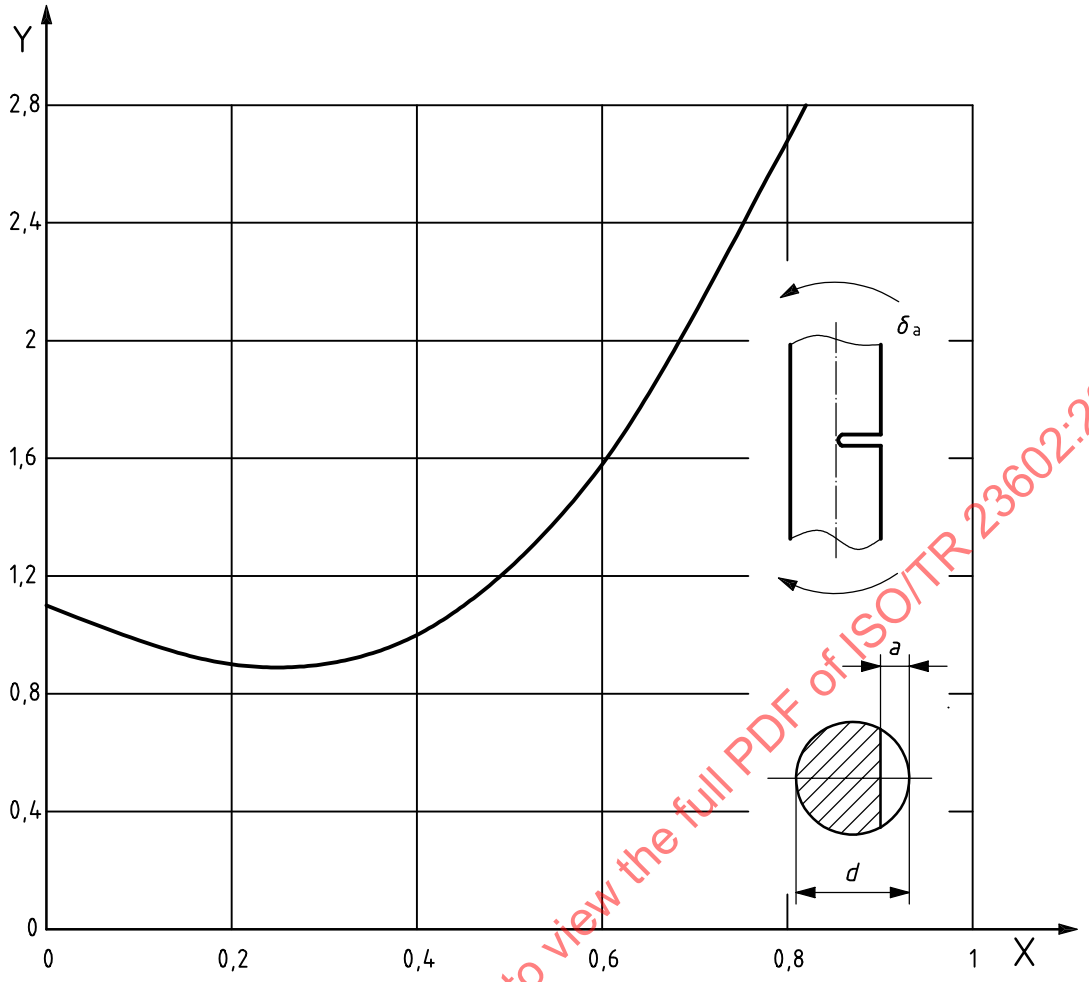

$$K_I = \sigma_b \sqrt{\Pi \cdot a \cdot F_i}$$

Key

X relative crack depth, a/d
Y correction factor, F_i

Figure 31 — Correction factor for long bending bars [5]